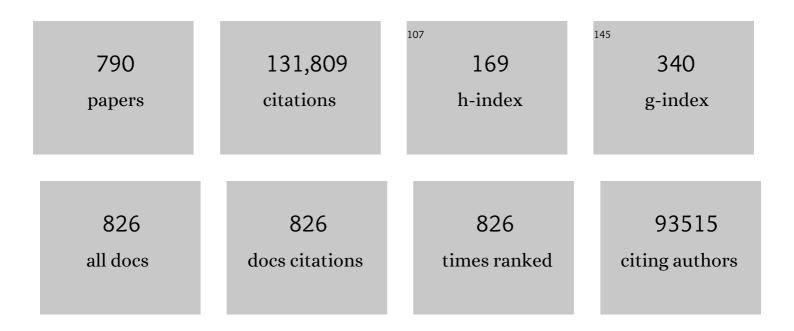
List of Publications by Year in descending order

Source: https://exaly.com/author-pdf/4975007/publications.pdf Version: 2024-02-01



HUIL-MING CHENC

#	Article	IF	CITATIONS
1	Homologous gradient heterostructureâ€based artificial synapses for neuromorphic computation. InformaAnÃ-Materiály, 2023, 5, .	8.5	6
2	Flexible organic photodetectors and their use in wearable systems. , 2022, 125, 103145.		13
3	Iron-doped NiS2 microcrystals with exposed {0 0 1} facets for electrocatalytic water oxidation. Journal of Colloid and Interface Science, 2022, 608, 599-604.	5.0	15
4	Response of microorganisms to phosphate nanoparticles in Pb polluted sediment: Implications of Pb bioavailability, enzyme activities and bacterial community. Chemosphere, 2022, 286, 131643.	4.2	15
5	Densification of MXene films by sequential bridging. National Science Review, 2022, 9, nwab195.	4.6	0
6	Grapheneâ€Supported Atomically Dispersed Metals as Bifunctional Catalysts for Nextâ€Generation Batteries Based on Conversion Reactions. Advanced Materials, 2022, 34, e2105812.	11.1	106
7	Structure-related electrochemical behavior of sulfur-rich polymer cathode with solid-solid conversion in lithium-sulfur batteries. Energy Storage Materials, 2022, 45, 1144-1152.	9.5	30
8	Synthesis of Carbon Nanotubes by Floating Catalyst Chemical Vapor Deposition and Their Applications. Advanced Functional Materials, 2022, 32, 2108541.	7.8	63
9	Challenges and development of lithium-ion batteries for low temperature environments. ETransportation, 2022, 11, 100145.	6.8	108
10	Construction of sandwich-structured C/C-SiC and C/C-SiC-ZrC composites with good mechanical and anti-ablation properties. Journal of the European Ceramic Society, 2022, 42, 1219-1226.	2.8	31
11	Lignocellulosic biomass derived N-doped and CoO-loaded carbocatalyst used as highly efficient peroxymonosulfate activator for ciprofloxacin degradation. Journal of Colloid and Interface Science, 2022, 610, 221-233.	5.0	17
12	Constructing a Stable Interface Layer by Tailoring Solvation Chemistry in Carbonate Electrolytes for Highâ€Performance Lithiumâ€Metal Batteries. Advanced Materials, 2022, 34, e2108400.	11.1	144
13	Kinetics-Controlled Growth of Metallic Single-Wall Carbon Nanotubes from CoRe <sub><i>x</i></sub> Nanoparticles. ACS Nano, 2022, 16, 232-240.	7.3	13
14	Uniform polypyrrole electrodeposition triggered by phytic acid-guided interface engineering for high energy density flexible supercapacitor. Journal of Colloid and Interface Science, 2022, 611, 356-365.	5.0	24
15	Metallic Co and crystalline Co-Mo oxides supported on graphite felt for bifunctional electrocatalytic hydrogen evolution and urea oxidation. Journal of Colloid and Interface Science, 2022, 612, 413-423.	5.0	30
16	An ultrathin and highly efficient interlayer for lithium–sulfur batteries with high sulfur loading and lean electrolyte. Journal of Materials Chemistry A, 2022, 10, 7653-7659.	5.2	33
17	2D Functional Minerals as Sustainable Materials for Magnetoâ€Optics. Advanced Materials, 2022, 34, e2110464.	11.1	26
18	3D Printed Templateâ€Directed Assembly of Multiscale Graphene Structures. Advanced Functional Materials, 2022, 32, .	7.8	18

#	Article	IF	CITATIONS
19	Electrochemical Deposition of a Singleâ€Crystalline Nanorod Polycyclic Aromatic Hydrocarbon Film with Efficient Charge and Exciton Transport. Angewandte Chemie, 2022, 134, .	1.6	3
20	Ultrastable Interfacial Contacts Enabling Unimpeded Charge Transfer and Ion Diffusion in Flexible Lithiumâ€lon Batteries. Advanced Science, 2022, 9, e2105419.	5.6	12
21	Effect of C/SiC Volume Ratios on Mechanical and Oxidation Behaviors of Cf/C–SiC Composites Fabricated by Chemical Vapor Infiltration Technique. Acta Metallurgica Sinica (English Letters), 2022, 35, 801-811.	1.5	3
22	Designing Electrophilic and Nucleophilic Dual Centers in the ReS <sub>2</sub> Plane toward Efficient Bifunctional Catalysts for Li-CO <sub>2</sub> Batteries. Journal of the American Chemical Society, 2022, 144, 3106-3116.	6.6	93
23	Electrochemical Deposition of a Singleâ€Crystalline Nanorod Polycyclic Aromatic Hydrocarbon Film with Efficient Charge and Exciton Transport. Angewandte Chemie - International Edition, 2022, 61, .	7.2	14
24	Kinetic regulation of MXene with water-in-LiCl electrolyte for high-voltage micro-supercapacitors. National Science Review, 2022, 9, .	4.6	39
25	Carrier Trapping in Wrinkled 2D Monolayer MoS <sub>2</sub> for Ultrathin Memory. ACS Nano, 2022, 16, 6309-6316.	7.3	22
26	Patterning of Waferâ€Scale MXene Films for Highâ€Performance Image Sensor Arrays. Advanced Materials, 2022, 34, e2201298.	11.1	26
27	Fabrication of Large Aerogel-Like Carbon/Carbon Composites with Excellent Load-Bearing Capacity and Thermal-Insulating Performance at 1800 ŰC. ACS Nano, 2022, 16, 6565-6577.	7.3	45
28	AÂ2D material–based transparent hydrogel with engineerable interference colours. Nature Communications, 2022, 13, 1212.	5.8	37
29	Enhancing hydrogen peroxide activation of Cu Co layered double hydroxide by compositing with biochar: Performance and mechanism. Science of the Total Environment, 2022, 828, 154188.	3.9	33
30	Accurate structural descriptor enabled screening for nitrogen and oxygen vacancy codoped TiO2 with a large bandgap narrowing. Journal of Materials Science and Technology, 2022, 122, 84-90.	5.6	8
31	Toward an Understanding of the Reversible Li-CO <sub>2</sub> Batteries over Metal–N <sub>4</sub> -Functionalized Graphene Electrocatalysts. ACS Nano, 2022, 16, 1523-1532.	7.3	52
32	Fabrication of Largeâ€Area Uniform Nanometerâ€Thick Functional Layers and Their Stacks for Flexible Quantum Dot Lightâ€Emitting Diodes. Small Methods, 2022, 6, e2101030.	4.6	3
33	Electrochemical Capacitors with Confined Redox Electrolytes and Porous Electrodes. Advanced Materials, 2022, 34, e2202380.	11.1	33
34	2D Functional Minerals as Sustainable Materials for Magnetoâ€Optics (Adv. Mater. 16/2022). Advanced Materials, 2022, 34, .	11.1	7
35	A potential link between the structure of iron catalysts and Fenton-like performance: from fundamental understanding to engineering design. Journal of Materials Chemistry A, 2022, 10, 12788-12804.	5.2	15
36	A nonflammable electrolyte for ultrahigh-voltage (4.8 V-class) Li    NCM811 cells with a wide temperature range of 100 ŰC. Energy and Environmental Science, 2022, 15, 2435-2444.	15.6	104

#	Article	IF	CITATIONS
37	A photon-controlled diode with a new signal-processing behavior. National Science Review, 2022, 9, .	4.6	2
38	Viscous Solvent-Assisted Planetary Ball Milling for the Scalable Production of Large Ultrathin Two-Dimensional Materials. ACS Nano, 2022, 16, 10179-10187.	7.3	26
39	Direct and green repairing of degraded LiCoO2 for reuse in lithium-ion batteries. National Science Review, 2022, 9, .	4.6	85
40	An Interlayer Containing Dissociated LiNO <sub>3</sub> with Fast Release Speed for Stable Lithium Metal Batteries with 400ÂWh kg <sup>â^'1</sup> Energy Density. Small, 2022, 18, .	5.2	14
41	Atomic‣cale Design of Anode Materials for Alkali Metal (Li/Na/K)â€lon Batteries: Progress and Perspectives. Advanced Energy Materials, 2022, 12, .	10.2	56
42	Tailoring microstructures of carbon fiber reinforced carbon aerogel-like matrix composites by carbonization to modulate their mechanical properties and thermal conductivities. Carbon, 2022, 196, 807-818.	5.4	19
43	Decoupling of ion pairing and ion conduction in ultrahigh-concentration electrolytes enables wide-temperature solid-state batteries. Energy and Environmental Science, 2022, 15, 3379-3387.	15.6	29
44	Engineering Graphene Grain Boundaries for Plasmonic Multi-Excitation and Hotspots. ACS Nano, 2022, 16, 9041-9048.	7.3	7
45	In-situ imaging techniques for advanced battery development. Materials Today, 2022, 57, 279-294.	8.3	16
46	Dual-metal precursors for the universal growth of non-layered 2D transition metal chalcogenides with ordered cation vacancies. Science Bulletin, 2022, 67, 1649-1658.	4.3	10
47	Electronic structure adjustment of lithium sulfide by a single-atom copper catalyst toward high-rate lithium-sulfur batteries. Energy Storage Materials, 2022, 51, 890-899.	9.5	52
48	Preparation of isolated semiconducting single-wall carbon nanotubes by oxygen-assisted floating catalyst chemical vapor deposition. Chemical Engineering Journal, 2022, 450, 137861.	6.6	7
49	Dissolution-precipitation growth of uniform and clean two dimensional transition metal dichalcogenides. National Science Review, 2021, 8, nwaa115.	4.6	42
50	Single-atom catalysts for metal-sulfur batteries: Current progress and future perspectives. Journal of Energy Chemistry, 2021, 54, 452-466.	7.1	63
51	In-situ self-assembly construction of hollow tubular g-C3N4 isotype heterojunction for enhanced visible-light photocatalysis: Experiments and theories. Journal of Hazardous Materials, 2021, 401, 123355.	6.5	157
52	Extremely efficient flexible organic solar cells with a graphene transparent anode: Dependence on number of layers and doping of graphene. Carbon, 2021, 171, 350-358.	5.4	33
53	Six-membered-ring inorganic materials: definition and prospects. National Science Review, 2021, 8, nwaa248.	4.6	14
54	Chemical Vapor Deposition Growth of Two-Dimensional Compound Materials: Controllability, Material Quality, and Growth Mechanism. Accounts of Materials Research, 2021, 2, 36-47.	5.9	111

#	Article	IF	CITATIONS
55	Structure, Preparation, and Applications of 2D Materialâ€Based Metal–Semiconductor Heterostructures. Small Structures, 2021, 2, 2000093.	6.9	71
56	The application of Zeolitic imidazolate frameworks (ZIFs) and their derivatives based materials for photocatalytic hydrogen evolution and pollutants treatment. Chemical Engineering Journal, 2021, 417, 127914.	6.6	62
57	Surface and interface engineering of two-dimensional bismuth-based photocatalysts for ambient molecule activation. Journal of Materials Chemistry A, 2021, 9, 196-233.	5.2	50
58	Carbon Dotsâ€Decorated Carbonâ€Based Metalâ€Free Catalysts for Electrochemical Energy Storage. Small, 2021, 17, e2002998.	5.2	27
59	Modulating Electronic Structure of Monolayer Transition Metal Dichalcogenides by Substitutional Nbâ€Doping. Advanced Functional Materials, 2021, 31, 2006941.	7.8	54
60	Insights into the deposition chemistry of Li ions in nonaqueous electrolyte for stable Li anodes. Chemical Society Reviews, 2021, 50, 3178-3210.	18.7	126
61	High-performance flexible resistive random access memory devices based on graphene oxidized with a perpendicular oxidation gradient. Nanoscale, 2021, 13, 2448-2455.	2.8	12
62	Efficient Reversible Conversion between MoS <sub>2</sub> and Mo/Na <sub>2</sub> S Enabled by Graphene‣upported Single Atom Catalysts. Advanced Materials, 2021, 33, e2007090.	11.1	108
63	Superconductivity and High-Pressure Performance of 2D Mo <sub>2</sub> C Crystals. Journal of Physical Chemistry Letters, 2021, 12, 2219-2225.	2.1	3
64	High-throughput screening and machine learning for the efficient growth of high-quality single-wall carbon nanotubes. Nano Research, 2021, 14, 4610-4615.	5.8	11
65	A Durable and Efficient Electrocatalyst for Saline Water Splitting with Current Density Exceeding 2000ÂmAÂcm <sup>â^2</sup> . Advanced Functional Materials, 2021, 31, 2010367.	7.8	102
66	A flexible ultrasensitive optoelectronic sensor array for neuromorphic vision systems. Nature Communications, 2021, 12, 1798.	5.8	198
67	Doping Concentration Modulation in Vanadium-Doped Monolayer Molybdenum Disulfide for Synaptic Transistors. ACS Nano, 2021, 15, 7340-7347.	7.3	53
68	Properties and photodetector applications of two-dimensional black arsenic phosphorus and black phosphorus. Science China Information Sciences, 2021, 64, 1.	2.7	35
69	Intercalated architecture of MA2Z4 family layered van der Waals materials with emerging topological, magnetic and superconducting properties. Nature Communications, 2021, 12, 2361.	5.8	199
70	Polymorph Evolution Mechanisms and Regulation Strategies of Lithium Metal Anode under Multiphysical Fields. Chemical Reviews, 2021, 121, 5986-6056.	23.0	165
71	Largely Tunable Magneto-Coloration of Monolayer 2D Materials via Size Tailoring. ACS Nano, 2021, 15, 9445-9452.	7.3	7
72	Fabrication of high-conductivity RGO film at a temperature lower than 1500 ºC by electrical current. Journal of Materials Science: Materials in Electronics, 2021, 32, 11727-11736.	1.1	1

#	Article	IF	CITATIONS
73	Catalystâ€Free Growth of Atomically Thin Bi <sub>2</sub> O <sub>2</sub> Se Nanoribbons for Highâ€Performance Electronics and Optoelectronics. Advanced Functional Materials, 2021, 31, 2101170.	7.8	23
74	Aligned Carbonâ€Based Electrodes for Fastâ€Charging Batteries: A Review. Small, 2021, 17, e2007676.	5.2	30
75	Engineering the Active Sites of Graphene Catalyst: From CO <sub>2</sub> Activation to Activate Li-CO <sub>2</sub> Batteries. ACS Nano, 2021, 15, 9841-9850.	7.3	71
76	An in-situ solidification strategy to block polysulfides in Lithium-Sulfur batteries. Energy Storage Materials, 2021, 37, 224-232.	9.5	55
77	Ionâ€Dipole Chemistry Drives Rapid Evolution of Li Ions Solvation Sheath in Lowâ€Temperature Li Batteries. Advanced Energy Materials, 2021, 11, 2100935.	10.2	95
78	Breaking the Rateâ€Integrity Dilemma in Largeâ€Area Bubbling Transfer of Graphene by Strain Engineering. Advanced Functional Materials, 2021, 31, 2104228.	7.8	7
79	Highâ€Performance ITOâ€Free Perovskite Solar Cells Enabled by Singleâ€Walled Carbon Nanotube Films. Advanced Functional Materials, 2021, 31, 2104396.	7.8	30
80	Anisotropic moiré optical transitions in twisted monolayer/bilayer phosphorene heterostructures. Nature Communications, 2021, 12, 3947.	5.8	33
81	Independent thickness and lateral size sorting of two-dimensional materials. Science China Materials, 2021, 64, 2739-2746.	3.5	4
82	An ultrasensitive molybdenum-based double-heterojunction phototransistor. Nature Communications, 2021, 12, 4094.	5.8	37
83	Dualâ€Phasic Carbon with Co Single Atoms and Nanoparticles as a Bifunctional Oxygen Electrocatalyst for Rechargeable Zn–Air Batteries. Advanced Functional Materials, 2021, 31, 2103360.	7.8	107
84	Lithium Metal Batteries: Ionâ€Dipole Chemistry Drives Rapid Evolution of Li Ions Solvation Sheath in Lowâ€Temperature Li Batteries (Adv. Energy Mater. 28/2021). Advanced Energy Materials, 2021, 11, 2170112.	10.2	14
85	Collective Behavior Induced Highly Sensitive Magneto-Optic Effect in 2D Inorganic Liquid Crystals. Journal of the American Chemical Society, 2021, 143, 12886-12893.	6.6	12
86	High-Performance Lithium Metal Batteries with a Wide Operating Temperature Range in Carbonate Electrolyte by Manipulating Interfacial Chemistry. ACS Energy Letters, 2021, 6, 3170-3179.	8.8	71
87	Realization of a non-markov chain in a single 2D mineral RRAM. Science Bulletin, 2021, 66, 1634-1640.	4.3	15
88	Nanoribbons: Catalystâ€Free Growth of Atomically Thin Bi <sub>2</sub> O <sub>2</sub> Se Nanoribbons for Highâ€Performance Electronics and Optoelectronics (Adv. Funct. Mater. 31/2021). Advanced Functional Materials, 2021, 31, 2170230.	7.8	2
89	Magnetic Doping Induced Superconductivity-to-Incommensurate Density Waves Transition in a 2D Ultrathin Cr-Doped Mo <sub>2</sub> C Crystal. ACS Nano, 2021, 15, 14938-14946.	7.3	7
90	A flexible nickel phthalocyanine resistive random access memory with multi-level data storage capability. Journal of Materials Science and Technology, 2021, 86, 151-157.	5.6	18

#	Article	IF	CITATIONS
91	Glue-assisted grinding exfoliation of large-size 2D materials for insulating thermal conduction and large-current-density hydrogen evolution. Materials Today, 2021, 51, 145-154.	8.3	58
92	A Scalable Artificial Neuron Based on Ultrathin Two-Dimensional Titanium Oxide. ACS Nano, 2021, 15, 15123-15131.	7.3	25
93	Engineering <i>dâ€p</i> Orbital Hybridization in Singleâ€Atom Metalâ€Embedded Threeâ€Dimensional Electrodes for Li–S Batteries. Advanced Materials, 2021, 33, e2105947.	11.1	209
94	Ultralight carbon fiber felt reinforced monolithic carbon aerogel composites with excellent thermal insulation performance. Carbon, 2021, 183, 525-529.	5.4	52
95	Stress release in high-capacity flexible lithium-ion batteries through nested wrinkle texturing of graphene. Journal of Energy Chemistry, 2021, 61, 243-249.	7.1	10
96	Fluorination-assisted preparation of self-supporting single-atom Fe-N-doped single-wall carbon nanotube film as bifunctional oxygen electrode for rechargeable Zn-Air batteries. Applied Catalysis B: Environmental, 2021, 294, 120239.	10.8	70
97	Hierarchical urchin-like amorphous carbon with Co-adding anchored on nickel foam: A free-standing electrode for advanced asymmetrical supercapacitors and adsorbed Pb (II). Journal of Colloid and Interface Science, 2021, 603, 58-69.	5.0	9
98	A Ta-TaS2 monolith catalyst with robust and metallic interface for superior hydrogen evolution. Nature Communications, 2021, 12, 6051.	5.8	112
99	Semiconductor nanochannels in metallic carbon nanotubes by thermomechanical chirality alteration. Science, 2021, 374, 1616-1620.	6.0	32
100	Strategies towards Lowâ€Cost Dualâ€Ion Batteries with High Performance. Angewandte Chemie - International Edition, 2020, 59, 3802-3832.	7.2	242
101	Transfer-free CVD graphene for highly sensitive glucose sensors. Journal of Materials Science and Technology, 2020, 37, 71-76.	5.6	28
102	Dualâ€Additive Assisted Chemical Vapor Deposition for the Growth of Mnâ€Doped 2D MoS <sub>2</sub> with Tunable Electronic Properties. Small, 2020, 16, e1903181.	5.2	54
103	Mass production of 2D materials by intermediate-assisted grinding exfoliation. National Science Review, 2020, 7, 324-332.	4.6	100
104	A highly active and durable electrocatalyst for large current density hydrogen evolution reaction. Science Bulletin, 2020, 65, 123-130.	4.3	58
105	High-efficiency and stable silicon heterojunction solar cells with lightly fluorinated single-wall carbon nanotube films. Nano Energy, 2020, 69, 104442.	8.2	28
106	Reconstructed transparent conductive layers of fluorine doped tin oxide for greatly weakened hysteresis and improved efficiency of perovskite solar cells. Chemical Communications, 2020, 56, 129-132.	2.2	5
107	Unsaturated Single Atoms on Monolayer Transition Metal Dichalcogenides for Ultrafast Hydrogen Evolution. ACS Nano, 2020, 14, 767-776.	7.3	106
108	Semiconductor-based photocatalysts for photocatalytic and photoelectrochemical water splitting: will we stop with photocorrosion?. Journal of Materials Chemistry A, 2020, 8, 2286-2322.	5.2	251

HUI-MING CHENG

#	Article	IF	CITATIONS
109	Intercalation-Induced Conversion Reactions Give High-Capacity Potassium Storage. ACS Nano, 2020, 14, 14026-14035.	7.3	42
110	Porous Graphene Materials: The Chemistry and Promising Applications of Graphene and Porous Graphene Materials (Adv. Funct. Mater. 41/2020). Advanced Functional Materials, 2020, 30, 2070275.	7.8	48
111	Pushing the conductance and transparency limit of monolayer graphene electrodes for flexible organic light-emitting diodes. Proceedings of the National Academy of Sciences of the United States of America, 2020, 117, 25991-25998.	3.3	28
112	Status and prospects of porous graphene networks for lithium–sulfur batteries. Materials Horizons, 2020, 7, 2487-2518.	6.4	63
113	Precise Identification of the Active Phase of Cobalt Catalyst for Carbon Nanotube Growth by <i>In Situ</i> Transmission Electron Microscopy. ACS Nano, 2020, 14, 16823-16831.	7.3	51
114	Chemical vapor deposition of layered two-dimensional MoSi <sub>2</sub> N <sub>4</sub> materials. Science, 2020, 369, 670-674.	6.0	556
115	Superhigh Uniform Magnetic Cr Substitution in a 2D Mo 2 C Superconductor for a Macroscopic cale Kondo Effect. Advanced Materials, 2020, 32, 2002825.	11.1	7
116	High-throughput production of cheap mineral-based two-dimensional electrocatalysts for high-current-density hydrogen evolution. Nature Communications, 2020, 11, 3724.	5.8	153
117	Giant magneto-birefringence effect and tuneable colouration of 2D crystal suspensions. Nature Communications, 2020, 11, 3725.	5.8	28
118	Megamerger of MOFs and g-C <sub>3</sub> N <sub>4</sub> for energy and environment applications: upgrading the framework stability and performance. Journal of Materials Chemistry A, 2020, 8, 17883-17906.	5.2	48
119	Synthesis of Ultrahighâ€Quality Monolayer Molybdenum Disulfide through In Situ Defect Healing with Thiol Molecules. Small, 2020, 16, e2003357.	5.2	36
120	CdPS <sub>3</sub> nanosheets-based membrane with high proton conductivity enabled by Cd vacancies. Science, 2020, 370, 596-600.	6.0	120
121	Distinct superconducting properties and hydrostatic pressure effects in 2D α- and β-Mo2C crystal sheets. NPG Asia Materials, 2020, 12, .	3.8	10
122	Homogeneous and Fast Ion Conduction of PEOâ€Based Solidâ€State Electrolyte at Low Temperature. Advanced Functional Materials, 2020, 30, 2007172.	7.8	246
123	The importance of H2 in the controlled growth of semiconducting single-wall carbon nanotubes. Journal of Materials Science and Technology, 2020, 54, 105-111.	5.6	9
124	Reliable liquid electrolytes for lithium metal batteries. Energy Storage Materials, 2020, 30, 113-129.	9.5	92
125	Critical review of recent progress of flexible perovskite solar cells. Materials Today, 2020, 39, 66-88.	8.3	169
126	Fast lithium ion transport in solid polymer electrolytes from polysulfide-bridged copolymers. Nano Energy, 2020, 75, 104976.	8.2	32

#	Article	IF	CITATIONS
127	Recent Progress in 3D Printing of 2D Materialâ€Based Macrostructures. Advanced Materials Technologies, 2020, 5, 1901066.	3.0	27
128	A flexible thermoelectric device based on a Bi2Te3-carbon nanotube hybrid. Journal of Materials Science and Technology, 2020, 58, 80-85.	5.6	31
129	Mechanical-electro-magnetic coupling in strained bilayer CrI3. Science China Technological Sciences, 2020, 63, 1265-1271.	2.0	3
130	3D graphene aerogel based photocatalysts: Synthesized, properties, and applications. Colloids and Surfaces A: Physicochemical and Engineering Aspects, 2020, 594, 124666.	2.3	24
131	Transport through a network of two-dimensional NbC superconducting crystals connected via weak links. Physical Review B, 2020, 101, .	1.1	2
132	The Chemistry and Promising Applications of Graphene and Porous Graphene Materials. Advanced Functional Materials, 2020, 30, 1909035.	7.8	181
133	Defect and interlayer coupling tuned quasiparticle scattering in 2D disordered Mo2C superconducting microcrystals. Journal Physics D: Applied Physics, 2020, 53, 434002.	1.3	1
134	Structure-related electrochemical performance of organosulfur compounds for lithium–sulfur batteries. Energy and Environmental Science, 2020, 13, 1076-1095.	15.6	143
135	An Anionâ€Tuned Solid Electrolyte Interphase with Fast Ion Transfer Kinetics for Stable Lithium Anodes. Advanced Energy Materials, 2020, 10, 1903843.	10.2	186
136	Second Time-Scale Synthesis of High-Quality Graphite Films by Quenching for Effective Electromagnetic Interference Shielding. ACS Nano, 2020, 14, 3121-3128.	7.3	57
137	Superhigh Electromagnetic Interference Shielding of Ultrathin Aligned Pristine Graphene Nanosheets Film. Advanced Materials, 2020, 32, e1907411.	11.1	310
138	Synthesis of monolithic carbon aerogels with high mechanical strength via ambient pressure drying without solvent exchange. Journal of Materials Science and Technology, 2020, 50, 66-74.	5.6	39
139	Bi-Cation Electrolyte for a 1.7 V Aqueous Zn Ion Battery. ACS Applied Materials & Interfaces, 2020, 12, 13790-13796.	4.0	78
140	Monolayer carbon-encapsulated Mo-doped Ni nanoparticles anchored on single-wall carbon nanotube film for total water splitting. Applied Catalysis B: Environmental, 2020, 269, 118823.	10.8	46
141	Metal sulfide/MOF-based composites as visible-light-driven photocatalysts for enhanced hydrogen production from water splitting. Coordination Chemistry Reviews, 2020, 409, 213220.	9.5	169
142	Ligand-assisted cation-exchange engineering for high-efficiency colloidal Cs1â^'xFAxPbI3 quantum dot solar cells with reduced phase segregation. Nature Energy, 2020, 5, 79-88.	19.8	412
143	A Flexible Carbon Nanotube Senâ€Memory Device. Advanced Materials, 2020, 32, e1907288.	11.1	48
144	A Nanosheet Array of Cu <sub>2</sub> Se Intercalation Compound with Expanded Interlayer Space for Sodium Ion Storage. Advanced Energy Materials, 2020, 10, 2000666.	10.2	67

#	Article	IF	CITATIONS
145	Sustainable hydrogen production by molybdenum carbide-based efficient photocatalysts: From properties to mechanism. Advances in Colloid and Interface Science, 2020, 279, 102144.	7.0	55
146	An integrated thermoelectric-assisted photoelectrochemical system to boost water splitting. Science Bulletin, 2020, 65, 1163-1169.	4.3	23
147	Vertical Chemical Vapor Deposition Growth of Highly Uniform 2D Transition Metal Dichalcogenides. ACS Nano, 2020, 14, 4646-4653.	7.3	101
148	Lithium Anodes: An Anionâ€Tuned Solid Electrolyte Interphase with Fast Ion Transfer Kinetics for Stable Lithium Anodes (Adv. Energy Mater. 14/2020). Advanced Energy Materials, 2020, 10, 2070063.	10.2	3
149	Carbon-Based Fibers for Advanced Electrochemical Energy Storage Devices. Chemical Reviews, 2020, 120, 2811-2878.	23.0	334
150	Electrochemical process of sulfur in carbon materials from electrode thickness to interlayer. Journal of Energy Chemistry, 2019, 31, 119-124.	7.1	42
151	Hollow Nanostructures for Photocatalysis: Advantages and Challenges. Advanced Materials, 2019, 31, e1801369.	11.1	506
152	The Regulating Role of Carbon Nanotubes and Graphene in Lithiumâ€Ion and Lithium–Sulfur Batteries. Advanced Materials, 2019, 31, e1800863.	11.1	339
153	High Yield Controlled Synthesis of Nano-Graphene Oxide by Water Electrolytic Oxidation of Glassy Carbon for Metal-Free Catalysis. ACS Nano, 2019, 13, 9482-9490.	7.3	25
154	High-performance single-wall carbon nanotube transparent conductive films. Journal of Materials Science and Technology, 2019, 35, 2447-2462.	5.6	51
155	Oriented outperforms disorder: Thickness-independent mass transport for lithium-sulfur batteries. Carbon, 2019, 154, 90-97.	5.4	12
156	Ultrafast growth of nanocrystalline graphene films by quenching and grain-size-dependent strength and bandgap opening. Nature Communications, 2019, 10, 4854.	5.8	43
157	Tunable In Situ Stress and Spontaneous Microwrinkling of Multiscale Heterostructures. Journal of Physical Chemistry C, 2019, 123, 26041-26046.	1.5	3
158	Allâ€Solidâ€State Planar Sodiumâ€ion Microcapacitors with Multidirectional Fast Ion Diffusion Pathways. Advanced Science, 2019, 6, 1902147.	5.6	34
159	Bottom-Up Synthesis of 2D Transition Metal Carbides and Nitrides. , 2019, , 89-109.		13
160	Improved Damping and High Strength of Graphene-Coated Nickel Hybrid Foams. ACS Applied Materials & Interfaces, 2019, 11, 42690-42696.	4.0	21
161	Micro-Macroscopic Coupled Electrode Architecture for High-Energy-Density Lithium–Sulfur Batteries. ACS Applied Energy Materials, 2019, 2, 7393-7402.	2.5	6
162	Perfect proton selectivity in ion transport through two-dimensional crystals. Nature Communications, 2019, 10, 4243.	5.8	60

#	Article	IF	CITATIONS
163	Production of carbon dots during the liquid phase exfoliation of MoS2 quantum dots. Carbon, 2019, 155, 243-249.	5.4	11
164	Suppressing lithium dendrite formation by slowing its desolvation kinetics. Chemical Communications, 2019, 55, 13211-13214.	2.2	43
165	Roles of multiwall carbon nanotubes in phytoremediation: cadmium uptake and oxidative burst in <i>Boehmeria nivea</i> (L.) Gaudich. Environmental Science: Nano, 2019, 6, 851-862.	2.2	34
166	Ultrahigh-voltage integrated micro-supercapacitors with designable shapes and superior flexibility. Energy and Environmental Science, 2019, 12, 1534-1541.	15.6	192
167	Die wiederaufladbare Aluminiumbatterie: Möglichkeiten und Herausforderungen. Angewandte Chemie, 2019, 131, 12104-12124.	1.6	26
168	Synthesis and applications of three-dimensional graphene network structures. Materials Today Nano, 2019, 5, 100027.	2.3	60
169	Carbonâ€Based Metalâ€Free Catalysts for Energy Storage and Environmental Remediation. Advanced Materials, 2019, 31, e1806128.	11.1	188
170	The Rechargeable Aluminum Battery: Opportunities and Challenges. Angewandte Chemie - International Edition, 2019, 58, 11978-11996.	7.2	276
171	A Desolvated Solid–Solid Interface for a Highâ€Capacitance Electric Double Layer. Advanced Energy Materials, 2019, 9, 1803715.	10.2	20
172	Engineering Two-Dimensional Materials and Their Heterostructures as High-Performance Electrocatalysts. Electrochemical Energy Reviews, 2019, 2, 373-394.	13.1	74
173	Smart Materials and Design toward Safe and Durable Lithium Ion Batteries. Small Methods, 2019, 3, 1900323.	4.6	47
174	Interlayer epitaxy of wafer-scale high-quality uniform AB-stacked bilayer graphene films on liquid Pt3Si/solid Pt. Nature Communications, 2019, 10, 2809.	5.8	43
175	Carbon nanotube-linked hollow carbon nanospheres doped with iron and nitrogen as single-atom catalysts for the oxygen reduction reaction in acidic solutions. Journal of Materials Chemistry A, 2019, 7, 14478-14482.	5.2	56
176	Carbon nanotube/silicon heterojunctions for photovoltaic applications. Nano Materials Science, 2019, 1, 156-172.	3.9	43
177	Secondary-Atom-Assisted Synthesis of Single Iron Atoms Anchored on N-Doped Carbon Nanowires for Oxygen Reduction Reaction. ACS Catalysis, 2019, 9, 5929-5934.	5.5	149
178	Energy band edge alignment of anisotropic BiVO4 to drive photoelectrochemical hydrogen evolution. Materials Today Energy, 2019, 13, 205-213.	2.5	12
179	An overview on nitride and nitrogen-doped photocatalysts for energy and environmental applications. Composites Part B: Engineering, 2019, 172, 704-723.	5.9	61
180	Gradient Sn-Doped Heteroepitaxial Film of Faceted Rutile TiO <sub>2</sub> as an Electron Selective Layer for Efficient Perovskite Solar Cells. ACS Applied Materials & Interfaces, 2019, 11, 19638-19646.	4.0	32

#	Article	IF	CITATIONS
181	Defective graphene as a high-efficiency Raman enhancement substrate. Journal of Materials Science and Technology, 2019, 35, 1996-2002.	5.6	13
182	A Double Support Layer for Facile Clean Transfer of Two-Dimensional Materials for High-Performance Electronic and Optoelectronic Devices. ACS Nano, 2019, 13, 5513-5522.	7.3	29
183	Quantifying the Volumetric Performance Metrics of Supercapacitors. Advanced Energy Materials, 2019, 9, 1900079.	10.2	88
184	Transfer Methods of Graphene from Metal Substrates: A Review. Small Methods, 2019, 3, 1900049.	4.6	67
185	A Freestanding Singleâ€Wall Carbon Nanotube Film Decorated with Nâ€Doped Carbonâ€Encapsulated Ni Nanoparticles as a Bifunctional Electrocatalyst for Overall Water Splitting. Advanced Science, 2019, 6, 1802177.	5.6	56
186	2D hierarchical yolk-shell heterostructures as advanced host-interlayer integrated electrode for enhanced Li-S batteries. Journal of Energy Chemistry, 2019, 36, 64-73.	7.1	39
187	Layer-Stacking, Defects, and Robust Superconductivity on the Mo-Terminated Surface of Ultrathin Mo <sub>2</sub> C Flakes Grown by CVD. Nano Letters, 2019, 19, 3327-3335.	4.5	21
188	Nickel phthalocyanine as an excellent hole-transport material in inverted planar perovskite solar cells. Chemical Communications, 2019, 55, 5343-5346.	2.2	25
189	Ultrafast Transition of Nonuniform Graphene to High-Quality Uniform Monolayer Films on Liquid Cu. ACS Applied Materials & Interfaces, 2019, 11, 17629-17636.	4.0	10
190	Towards the practical use of flexible lithium ion batteries. Energy Storage Materials, 2019, 23, 434-438.	9.5	73
191	Multifunctional fabrics of carbon nanotube fibers. Journal of Materials Chemistry A, 2019, 7, 8790-8797.	5.2	54
192	Identification of active sites in nitrogen and sulfur co-doped carbon-based oxygen reduction catalysts. Carbon, 2019, 147, 303-311.	5.4	44
193	Boosting photoelectrochemical water splitting performance of Ta3N5 nanorod array photoanodes by forming a dual co-catalyst shell. Nano Energy, 2019, 59, 683-688.	8.2	52
194	Fabrication of novel magnetic MnFe2O4/bio-char composite and heterogeneous photo-Fenton degradation of tetracycline in near neutral pH. Chemosphere, 2019, 224, 910-921.	4.2	287
195	Electric Double Layer: A Desolvated Solid–Solid Interface for a High apacitance Electric Double Layer (Adv. Energy Mater. 12/2019). Advanced Energy Materials, 2019, 9, 1970037.	10.2	3
196	Water-assisted rapid growth of monolayer graphene films on SiO2/Si substrates. Carbon, 2019, 148, 241-248.	5.4	35
197	Synergistic Effect of Aligned Graphene Nanosheets in Graphene Foam for Highâ€₽erformance Thermally Conductive Composites. Advanced Materials, 2019, 31, e1900199.	11.1	173
198	Overview of the synthesis of MXenes and other ultrathin 2D transition metal carbides and nitrides. Current Opinion in Solid State and Materials Science, 2019, 23, 149-163.	5.6	353

#	Article	IF	CITATIONS
199	Effects of domain structures on vortex state of two-dimensional superconducting Mo <sub>2</sub> C crystals. 2D Materials, 2019, 6, 021005.	2.0	8
200	Mitigating self-discharge of carbon-based electrochemical capacitors by modifying their electric-double layer to maximize energy efficiency. Journal of Energy Chemistry, 2019, 38, 214-218.	7.1	31
201	Supercapacitors: Silicaâ€Mediated Formation of Nickel Sulfide Nanosheets on CNT Films for Versatile Energy Storage (Small 15/2019). Small, 2019, 15, 1970081.	5.2	2
202	Homogeneous Doping of Substitutional Nitrogen/Carbon in TiO <sub>2</sub> Plates for Visible Light Photocatalytic Water Oxidation. Advanced Functional Materials, 2019, 29, 1901943.	7.8	61
203	Key Aspects of Lithium Metal Anodes for Lithium Metal Batteries. Small, 2019, 15, e1900687.	5.2	253
204	Free-standing integrated cathode derived from 3D graphene/carbon nanotube aerogels serving as binder-free sulfur host and interlayer for ultrahigh volumetric-energy-density lithium sulfur batteries. Nano Energy, 2019, 60, 743-751.	8.2	151
205	Chlorine capped SnO2 quantum-dots modified TiO2 electron selective layer to enhance the performance of planar perovskite solar cells. Science Bulletin, 2019, 64, 547-552.	4.3	32
206	Controlled Vapor–Solid Deposition of Millimeter‣ize Single Crystal 2D Bi <sub>2</sub> O <sub>2</sub> Se for Highâ€Performance Phototransistors. Advanced Functional Materials, 2019, 29, 1807979.	7.8	143
207	Vertically aligned carbon nanotube arrays as a thermal interface material. APL Materials, 2019, 7, .	2.2	43
208	Lithium Batteries: The Regulating Role of Carbon Nanotubes and Graphene in Lithium–Ion and Lithium–Sulfur Batteries (Adv. Mater. 9/2019). Advanced Materials, 2019, 31, 1970066.	11.1	8
209	Silicaâ€Mediated Formation of Nickel Sulfide Nanosheets on CNT Films for Versatile Energy Storage. Small, 2019, 15, e1805064.	5.2	45
210	Preparation of metallic single-wall carbon nanotubes. Carbon, 2019, 147, 187-198.	5.4	22
211	Artificial Z-scheme photocatalytic system: What have been done and where to go?. Coordination Chemistry Reviews, 2019, 385, 44-80.	9.5	265
212	Transport Properties of Topological Semimetal Tungsten Carbide in the 2D Limit. Advanced Electronic Materials, 2019, 5, 1800839.	2.6	5
213	Strategies for Modifying TiO <sub>2</sub> Based Electron Transport Layers to Boost Perovskite Solar Cells. ACS Sustainable Chemistry and Engineering, 2019, 7, 4586-4618.	3.2	83
214	Integrated Paper-Based Flexible Li-Ion Batteries Made by a Rod Coating Method. ACS Applied Materials & Interfaces, 2019, 11, 46776-46782.	4.0	19
215	Megamerger in photocatalytic field: 2D g-C3N4 nanosheets serve as support of 0D nanomaterials for improving photocatalytic performance. Applied Catalysis B: Environmental, 2019, 240, 153-173.	10.8	310
216	Controllable edge modification of multi-layer graphene for improved dispersion stability and high electrical conductivity. Applied Nanoscience (Switzerland), 2019, 9, 469-477.	1.6	8

#	Article	IF	CITATIONS
217	A highly reversible Co3S4 microsphere cathode material for aluminum-ion batteries. Nano Energy, 2019, 56, 100-108.	8.2	179
218	Flexible layer-structured Bi2Te3 thermoelectric on a carbon nanotube scaffold. Nature Materials, 2019, 18, 62-68.	13.3	316
219	Insights into the effect of chemical treatment on the physicochemical characteristics and adsorption behavior of pig manure-derived biochars. Environmental Science and Pollution Research, 2019, 26, 1962-1972.	2.7	7
220	Morphology and surface chemistry engineering toward pH-universal catalysts for hydrogen evolution at high current density. Nature Communications, 2019, 10, 269.	5.8	431
221	Simultaneous Production and Functionalization of Boron Nitride Nanosheets by Sugarâ€Assisted Mechanochemical Exfoliation. Advanced Materials, 2019, 31, e1804810.	11.1	220
222	Grain Boundaries and Tilt-Angle-Dependent Transport Properties of a 2D Mo <sub>2</sub> C Superconductor. Nano Letters, 2019, 19, 857-865.	4.5	18
223	Long-term oxidation behaviors of C/SiC composites with a SiC/UHTC/SiC three-layer coating in a wide temperature range. Corrosion Science, 2019, 147, 1-8.	3.0	46
224	Control of Spatially Homogeneous Distribution of Heteroatoms to Produce Red TiO <sub>2</sub> Photocatalyst for Visible‣ight Photocatalytic Water Splitting. Chemistry - A European Journal, 2019, 25, 1787-1794.	1.7	30
225	The effect of Pt nanoparticles distribution on the removal of cyanide by TiO2 coated Al-MCM-41 in blue light exposure. Arabian Journal of Chemistry, 2019, 12, 957-965.	2.3	18
226	Confined van der Waals Epitaxial Growth of Two-Dimensional Large Single-Crystal In <sub>2</sub> Se <sub>3</sub> for Flexible Broadband Photodetectors. Research, 2019, 2019, 1-10.	2.8	20
227	Confined van der Waals Epitaxial Growth of Two-Dimensional Large Single-Crystal In <sub>2</sub> Se <sub>3</sub> for Flexible Broadband Photodetectors. Research, 2019, 2019, 2763704.	2.8	18
228	Metal–Organic Frameworks (MOFs)â€Derived Nitrogenâ€Doped Porous Carbon Anchored on Graphene with Multifunctional Effects for Lithium–Sulfur Batteries. Advanced Functional Materials, 2018, 28, 1707592.	7.8	246
229	Highâ€Throughput Fabrication of Flexible and Transparent Allâ€Carbon Nanotube Electronics. Advanced Science, 2018, 5, 1700965.	5.6	34
230	A 3D Multifunctional Architecture for Lithium–Sulfur Batteries with High Areal Capacity. Small Methods, 2018, 2, 1800067.	4.6	33
231	Reversible calcium alloying enables a practical room-temperature rechargeable calcium-ion battery with a high discharge voltage. Nature Chemistry, 2018, 10, 667-672.	6.6	971
232	Two-Dimensional MoS <sub>2</sub> Confined Co(OH) <sub>2</sub> Electrocatalysts for Hydrogen Evolution in Alkaline Electrolytes. ACS Nano, 2018, 12, 4565-4573.	7.3	302
233	Highly stable graphene-oxide-based membranes with superior permeability. Nature Communications, 2018, 9, 1486.	5.8	428
234	Selective Chemical Epitaxial Growth of TiO2 Islands on Ferroelectric PbTiO3 Crystals to Boost Photocatalytic Activity. Joule, 2018, 2, 1095-1107.	11.7	113

#	Article	IF	CITATIONS
235	Ultrathin 2D Transition Metal Carbides for Ultrafast Pulsed Fiber Lasers. ACS Photonics, 2018, 5, 1808-1816.	3.2	148
236	Noninvasively Modifying Band Structures of Wideâ€Bandgap Metal Oxides to Boost Photocatalytic Activity. Advanced Materials, 2018, 30, e1706259.	11.1	48
237	Two-Dimensional Materials for Thermal Management Applications. Joule, 2018, 2, 442-463.	11.7	353
238	Degradation of di (2-ethylhexyl) phthalate in sediment by a surfactant-enhanced Fenton-like process. Chemosphere, 2018, 198, 327-333.	4.2	17
239	In Situ Grown Agl/Bi <sub>12</sub> O <sub>17</sub> Cl <sub>2</sub> Heterojunction Photocatalysts for Visible Light Degradation of Sulfamethazine: Efficiency, Pathway, and Mechanism. ACS Sustainable Chemistry and Engineering, 2018, 6, 4174-4184.	3.2	249
240	Chemical Vapor Deposition Growth and Applications of Two-Dimensional Materials and Their Heterostructures. Chemical Reviews, 2018, 118, 6091-6133.	23.0	1,000
241	Atomically Dispersed Transition Metals on Carbon Nanotubes with Ultrahigh Loading for Selective Electrochemical Carbon Dioxide Reduction. Advanced Materials, 2018, 30, e1706287.	11.1	459
242	An Aluminum–Sulfur Battery with a Fast Kinetic Response. Angewandte Chemie, 2018, 130, 1916-1920.	1.6	43
243	An Aluminum–Sulfur Battery with a Fast Kinetic Response. Angewandte Chemie - International Edition, 2018, 57, 1898-1902.	7.2	154
244	A gradient bi-functional graphene-based modified electrode for vanadium redox flow batteries. Energy Storage Materials, 2018, 13, 66-71.	9.5	84
245	N-doped carbon nanotubes containing a high concentration of single iron atoms for efficient oxygen reduction. NPG Asia Materials, 2018, 10, e461-e461.	3.8	103
246	An Unusual Strong Visibleâ€Light Absorption Band in Red Anatase TiO <sub>2</sub> Photocatalyst Induced by Atomic Hydrogenâ€Occupied Oxygen Vacancies. Advanced Materials, 2018, 30, 1704479.	11.1	231
247	Green synthesis of graphene oxide byÂseconds timescale water electrolytic oxidation. Nature Communications, 2018, 9, 145.	5.8	468
248	Selective growth of semiconducting single-wall carbon nanotubes using SiC as a catalyst. Carbon, 2018, 135, 195-201.	5.4	11
249	A Rechargeable Quasi-symmetrical MoS2 Battery. Joule, 2018, 2, 1278-1286.	11.7	33
250	Ultrahigh-performance transparent conductive films of carbon-welded isolated single-wall carbon nanotubes. Science Advances, 2018, 4, eaap9264.	4.7	178
251	Substitutional Carbonâ€Modified Anatase TiO <sub>2</sub> Decahedral Plates Directly Derived from Titanium Oxalate Crystals via Topotactic Transition. Advanced Materials, 2018, 30, e1705999.	11.1	46
252	Clean, fast and scalable transfer of ultrathin/patterned vertically-aligned carbon nanotube arrays. Carbon, 2018, 133, 275-282.	5.4	21

#	Article	IF	CITATIONS
253	Computational design and property predictions for two-dimensional nanostructures. Materials Today, 2018, 21, 391-418.	8.3	78
254	Homogeneous boron doping in a TiO2 shell supported on a TiB2 core for enhanced photocatalytic water oxidation. Chinese Journal of Catalysis, 2018, 39, 431-437.	6.9	8
255	Maximizing the visible light photoelectrochemical activity of B/N-doped anatase TiO2 microspheres with exposed dominant {001} facets. Science China Materials, 2018, 61, 831-838.	3.5	22
256	Boosting efficiency and stability of perovskite solar cells with nickel phthalocyanine as a low-cost hole transporting layer material. Journal of Materials Science and Technology, 2018, 34, 1474-1480.	5.6	45
257	Improving the photocatalytic activity of graphitic carbon nitride by thermal treatment in a high-pressure hydrogen atmosphere. Progress in Natural Science: Materials International, 2018, 28, 183-188.	1.8	31
258	Tween 80 surfactant-enhanced bioremediation: toward a solution to the soil contamination by hydrophobic organic compounds. Critical Reviews in Biotechnology, 2018, 38, 17-30.	5.1	80
259	Arch-inspired super-elastic carbon materials. National Science Review, 2018, 5, 3-4.	4.6	0
260	Mass production and industrial applications of graphene materials. National Science Review, 2018, 5, 90-101.	4.6	222
261	Remediation of contaminated soils by biotechnology with nanomaterials: bio-behavior, applications, and perspectives. Critical Reviews in Biotechnology, 2018, 38, 455-468.	5.1	158
262	Molecular docking simulation on the interactions of laccase from Trametes versicolor with nonylphenol and octylphenol isomers. Bioprocess and Biosystems Engineering, 2018, 41, 331-343.	1.7	30
263	Iron Oxide Nanoclusters Incorporated into Iron Phthalocyanine as Highly Active Electrocatalysts for the Oxygen Reduction Reaction. ChemCatChem, 2018, 10, 475-483.	1.8	18
264	Polysulfide immobilization and conversion on a conductive polar MoC@MoOx material for lithium-sulfur batteries. Energy Storage Materials, 2018, 10, 56-61.	9.5	157
265	Lithiumâ€Sulfur Batteries: Metal–Organic Frameworks (MOFs)â€Derived Nitrogenâ€Doped Porous Carbon Anchored on Graphene with Multifunctional Effects for Lithium–Sulfur Batteries (Adv. Funct. Mater.) Tj ETQq1 I	l <b>0.</b> 88431	'4 <b>₄g</b> BT /Over
266	Carbon Nanotubes and Related Nanomaterials: Critical Advances and Challenges for Synthesis toward Mainstream Commercial Applications. ACS Nano, 2018, 12, 11756-11784.	7.3	388
267	UV-Epoxy-Enabled Simultaneous Intact Transfer and Highly Efficient Doping for Roll-to-Roll Production of High-Performance Graphene Films. ACS Applied Materials & Interfaces, 2018, 10, 40756-40763.	4.0	18
268	A MnO2 nanosheet/single-wall carbon nanotube hybrid fiber for wearable solid-state supercapacitors. Carbon, 2018, 140, 634-643.	5.4	48
269	Efficient and scalable synthesis of highly aligned and compact two-dimensional nanosheet films with record performances. Nature Communications, 2018, 9, 3484.	5.8	165
270	Controlling reduction degree of graphene oxide membranes for improved water permeance. Science Bulletin, 2018, 63, 788-794.	4.3	131

#	Article	IF	CITATIONS
271	CuS Microspheres with Tunable Interlayer Space and Micropore as a Highâ€Rate and Longâ€Life Anode for Sodiumâ€Ion Batteries. Advanced Energy Materials, 2018, 8, 1800930.	10.2	183
272	All-solid-state flexible planar lithium ion micro-capacitors. Energy and Environmental Science, 2018, 11, 2001-2009.	15.6	160
273	Graphitic Carbon Nitride-Based Heterojunction Photoactive Nanocomposites: Applications and Mechanism Insight. ACS Applied Materials & Interfaces, 2018, 10, 21035-21055.	4.0	266
274	Facile Hydrothermal Synthesis of <i>Z</i> -Scheme Bi <sub>2</sub> Fe <sub>4</sub> O <sub>9</sub> /Bi <sub>2</sub> WO <sub>6</sub> Heterojunction Photocatalyst with Enhanced Visible Light Photocatalytic Activity. ACS Applied Materials & amp; Interfaces, 2018, 10, 18824-18836.	4.0	397
275	Continuous Fabrication of Meterâ€Scale Singleâ€Wall Carbon Nanotube Films and their Use in Flexible and Transparent Integrated Circuits. Advanced Materials, 2018, 30, e1802057.	11.1	63
276	Chirality transitions and transport properties of individual few-walled carbon nanotubes as revealed by in situ TEM probing. Ultramicroscopy, 2018, 194, 108-116.	0.8	9
277	Unique physicochemical properties of two-dimensional light absorbers facilitating photocatalysis. Chemical Society Reviews, 2018, 47, 6410-6444.	18.7	178
278	Singleâ€Atom Catalysts: Atomically Dispersed Transition Metals on Carbon Nanotubes with Ultrahigh Loading for Selective Electrochemical Carbon Dioxide Reduction (Adv. Mater. 13/2018). Advanced Materials, 2018, 30, 1870088.	11.1	8
279	Reduced graphene oxide/metal oxide nanoparticles composite membranes for highly efficient molecular separation. Journal of Materials Science and Technology, 2018, 34, 1481-1486.	5.6	79
280	The effect of carbon support on the oxygen reduction activity and durability of single-atom iron catalysts. MRS Communications, 2018, 8, 1158-1166.	0.8	27
281	Small-bundle single-wall carbon nanotubes for high-efficiency silicon heterojunction solar cells. Nano Energy, 2018, 50, 521-527.	8.2	43
282	NiPS <sub>3</sub> Nanosheet–Graphene Composites as Highly Efficient Electrocatalysts for Oxygen Evolution Reaction. ACS Nano, 2018, 12, 5297-5305.	7.3	104
283	Preparation of 2D material dispersions and their applications. Chemical Society Reviews, 2018, 47, 6224-6266.	18.7	459
284	Structural Control of Graphene-Based Materials for Unprecedented Performance. ACS Nano, 2018, 12, 5085-5092.	7.3	50
285	Carbon nanotube encapsulated in nitrogen and phosphorus co-doped carbon as a bifunctional electrocatalyst for oxygen reduction and evolution reactions. Carbon, 2018, 139, 156-163.	5.4	97
286	Development of Graphene-based Materials for Lithium-Sulfur Batteries. Wuli Huaxue Xuebao/ Acta Physico - Chimica Sinica, 2018, 34, 377-390.	2.2	26
287	WB crystals with oxidized surface as counter electrode in dye-sensitized solar cells. Science Bulletin, 2017, 62, 114-118.	4.3	10
288	Rosin-enabled ultraclean and damage-free transfer of graphene for large-area flexible organic light-emitting diodes. Nature Communications, 2017, 8, 14560.	5.8	184

#	Article	IF	CITATIONS
289	The rapid degradation of bisphenol A induced by the response of indigenous bacterial communities in sediment. Applied Microbiology and Biotechnology, 2017, 101, 3919-3928.	1.7	34
290	Effects of calcium at toxic concentrations of cadmium in plants. Planta, 2017, 245, 863-873.	1.6	169
291	Tailoring the thermal and electrical transport properties of graphene films by grain size engineering. Nature Communications, 2017, 8, 14486.	5.8	154
292	Circular Graphene Platelets with Grain Size and Orientation Gradients Grown by Chemical Vapor Deposition. Advanced Materials, 2017, 29, 1605451.	11.1	8
293	Arbitrary-Shaped Graphene-Based Planar Sandwich Supercapacitors on One Substrate with Enhanced Flexibility and Integration. ACS Nano, 2017, 11, 2171-2179.	7.3	121
294	Conductive porous vanadium nitride/graphene composite as chemical anchor of polysulfides for lithium-sulfur batteries. Nature Communications, 2017, 8, 14627.	5.8	912
295	Cadmium-containing quantum dots: properties, applications, and toxicity. Applied Microbiology and Biotechnology, 2017, 101, 2713-2733.	1.7	102
296	Effects of edge on graphene plasmons as revealed by infrared nanoimaging. Light: Science and Applications, 2017, 6, e16204-e16204.	7.7	68
297	Biological technologies for the remediation of co-contaminated soil. Critical Reviews in Biotechnology, 2017, 37, 1062-1076.	5.1	423
298	Graphene: a promising 2D material for electrochemical energy storage. Science Bulletin, 2017, 62, 724-740.	4.3	198
299	Charge delivery goes the distance. Science, 2017, 356, 582-583.	6.0	96
300	A carbon nanotube non-volatile memory device using a photoresist gate dielectric. Carbon, 2017, 124, 700-707.	5.4	10
301	Chitosan-wrapped gold nanoparticles for hydrogen-bonding recognition and colorimetric determination of the antibiotic kanamycin. Mikrochimica Acta, 2017, 184, 2097-2105.	2.5	79
302	Phase transition and in situ construction of lateral heterostructure of 2D superconducting α/β Mo <sub>2</sub> C with sharp interface by electron beam irradiation. Nanoscale, 2017, 9, 7501-7507.	2.8	28
303	Surface-restrained growth of vertically aligned carbon nanotube arrays with excellent thermal transport performance. Nanoscale, 2017, 9, 8213-8219.	2.8	17
304	Selective Growth of Metalâ€Free Metallic and Semiconducting Singleâ€Wall Carbon Nanotubes. Advanced Materials, 2017, 29, 1605719.	11.1	21
305	One-Step Device Fabrication of Phosphorene and Graphene Interdigital Micro-Supercapacitors with High Energy Density. ACS Nano, 2017, 11, 7284-7292.	7.3	312
306	Ultrafast Growth of Highâ€Quality Monolayer WSe <sub>2</sub> on Au. Advanced Materials, 2017, 29, 1700990.	11.1	139

#	Article	IF	CITATIONS
307	Strongly Coupled High-Quality Graphene/2D Superconducting Mo <sub>2</sub> C Vertical Heterostructures with Aligned Orientation. ACS Nano, 2017, 11, 5906-5914.	7.3	110
308	More Reliable Lithiumâ€&ulfur Batteries: Status, Solutions and Prospects. Advanced Materials, 2017, 29, 1606823.	11.1	1,414
309	Scalable Fabrication of Photochemically Reduced Graphene-Based Monolithic Micro-Supercapacitors with Superior Energy and Power Densities. ACS Nano, 2017, 11, 4283-4291.	7.3	176
310	A Sulfurâ€Rich Copolymer@CNT Hybrid Cathode with Dualâ€Confinement of Polysulfides for Highâ€Performance Lithium–Sulfur Batteries. Advanced Materials, 2017, 29, 1603835.	11.1	202
311	Single-wall carbon nanotube network enabled ultrahigh sulfur-content electrodes for high-performance lithium-sulfur batteries. Nano Energy, 2017, 42, 205-214.	8.2	183
312	On Energy: Electrochemical capacitors: Capacitance, functionality, and beyond. Energy Storage Materials, 2017, 9, A1-A3.	9.5	11
313	H2S + SO2 produces water-dispersed sulfur nanoparticles for lithium-sulfur batteries. Nano Energy, 2017, 41, 665-673.	8.2	12
314	Half-Metallicity in Co-Doped WSe <sub>2</sub> Nanoribbons. ACS Applied Materials & Interfaces, 2017, 9, 38796-38801.	4.0	17
315	Sandwich-structured C/C-SiC composites fabricated by electromagnetic-coupling chemical vapor infiltration. Scientific Reports, 2017, 7, 13120.	1.6	17
316	Stabilized Nanoscale Zerovalent Iron Mediated Cadmium Accumulation and Oxidative Damage of <i>Boehmeria nivea</i> (L.) Gaudich Cultivated in Cadmium Contaminated Sediments. Environmental Science & Technology, 2017, 51, 11308-11316.	4.6	248
317	A high tenacity electrode by assembly of a soft sorbent and a hard skeleton for lithium–sulfur batteries. Journal of Materials Chemistry A, 2017, 5, 22459-22464.	5.2	10
318	Comprehensive evaluation of the cytotoxicity of CdSe/ZnS quantum dots in Phanerochaete chrysosporium by cellular uptake and oxidative stress. Environmental Science: Nano, 2017, 4, 2018-2029.	2.2	81
319	Nitrogenâ€Superdoped 3D Graphene Networks for Highâ€Performance Supercapacitors. Advanced Materials, 2017, 29, 1701677.	11.1	230
320	Metre-size single-crystal graphene becomes a reality. Science Bulletin, 2017, 62, 1039-1040.	4.3	7
321	Magnetotransport in Ultrathin 2-D Superconducting Mo2C Crystals. IEEE Transactions on Magnetics, 2017, 53, 1-4.	1.2	9
322	High-Performance Sub-Micrometer Channel WSe <sub>2</sub> Field-Effect Transistors Prepared Using a Flood–Dike Printing Method. ACS Nano, 2017, 11, 12536-12546.	7.3	7
323	Growth of nanocarbons by catalysis and their applications. MRS Bulletin, 2017, 42, 790-793.	1.7	4
324	Applications of carbon nanotubes and graphene produced by chemical vapor deposition. MRS Bulletin, 2017, 42, 825-833.	1.7	14

#	Article	IF	CITATIONS
325	Carbon-encapsulated NiO nanoparticle decorated single-walled carbon nanotube thin films for binderless flexible electrodes of supercapacitors. Journal of Materials Chemistry A, 2017, 5, 24813-24819.	5.2	25
326	Air-stable and freestanding lithium alloy/graphene foil as an alternative to lithium metal anodes. Nature Nanotechnology, 2017, 12, 993-999.	15.6	376
327	Manganese-enhanced degradation of lignocellulosic waste by Phanerochaete chrysosporium: evidence of enzyme activity and gene transcription. Applied Microbiology and Biotechnology, 2017, 101, 6541-6549.	1.7	21
328	Phosphorene as a Polysulfide Immobilizer and Catalyst in Highâ€Performance Lithium–Sulfur Batteries. Advanced Materials, 2017, 29, 1602734.	11.1	289
329	Graphene-based materials for high-voltage and high-energy asymmetric supercapacitors. Energy Storage Materials, 2017, 6, 70-97.	9.5	260
330	Flexible batteries ahead. National Science Review, 2017, 4, 20-23.	4.6	35
331	Efficient organic photovoltaic cells on a single layer graphene transparent conductive electrode using MoO <sub>x</sub> as an interfacial layer. Nanoscale, 2017, 9, 251-257.	2.8	26
332	Carbon Nanotubes and Graphene for Flexible Electrochemical Energy Storage: from Materials to Devices. Advanced Materials, 2016, 28, 4306-4337.	11.1	595
333	Stabilizing sulfur cathodes using nitrogen-doped graphene as a chemical immobilizer for Li S batteries. Carbon, 2016, 108, 120-126.	5.4	134
334	Scalable Clean Exfoliation of Highâ€Quality Few‣ayer Black Phosphorus for a Flexible Lithium Ion Battery. Advanced Materials, 2016, 28, 510-517.	11.1	336
335	Ultra-thick graphene bulk supercapacitor electrodes for compact energy storage. Energy and Environmental Science, 2016, 9, 3135-3142.	15.6	347
336	Magnetotransport Properties in High-Quality Ultrathin Two-Dimensional Superconducting Mo <sub>2</sub> C Crystals. ACS Nano, 2016, 10, 4504-4510.	7.3	69
337	Controlled Growth of Semiconducting and Metallic Single-Wall Carbon Nanotubes. Journal of the American Chemical Society, 2016, 138, 6690-6698.	6.6	77
338	Understanding the interactions between lithium polysulfides and N-doped graphene using density functional theory calculations. Nano Energy, 2016, 25, 203-210.	8.2	347
339	A combined biological removal of Cd2+ from aqueous solutions using Phanerochaete chrysosporium and rice straw. Ecotoxicology and Environmental Safety, 2016, 130, 87-92.	2.9	18
340	Graphene oxide/graphene vertical heterostructure electrodes for highly efficient and flexible organic light emitting diodes. Nanoscale, 2016, 8, 10714-10723.	2.8	49
341	Kinetically Enhanced Electrochemical Redox of Polysulfides on Polymeric Carbon Nitrides for Improved Lithium–Sulfur Batteries. ACS Applied Materials & Interfaces, 2016, 8, 25193-25201.	4.0	149
342	Allâ€Carbon Thinâ€Film Transistors as a Step Towards Flexible and Transparent Electronics. Advanced Electronic Materials, 2016, 2, 1600229.	2.6	32

#	Article	IF	CITATIONS
343	Synthesis and Electrochemical Lithium Storage Behavior of Carbon Nanotubes Filled with Iron Sulfide Nanoparticles. Advanced Science, 2016, 3, 1600113.	5.6	44
344	Hierarchically porous Fe-N-doped carbon nanotubes as efficient electrocatalyst for oxygen reduction. Carbon, 2016, 109, 632-639.	5.4	74
345	An integrated electrode/separator with nitrogen and nickel functionalized carbon hybrids for advanced lithium/polysulfide batteries. Carbon, 2016, 109, 719-726.	5.4	55
346	A 3D bi-functional porous N-doped carbon microtube sponge electrocatalyst for oxygen reduction and oxygen evolution reactions. Energy and Environmental Science, 2016, 9, 3079-3084.	15.6	260
347	Toward More Reliable Lithium–Sulfur Batteries: An All-Graphene Cathode Structure. ACS Nano, 2016, 10, 8676-8682.	7.3	246
348	Mobility controlled linear magnetoresistance with 3D anisotropy in a layered graphene pallet. Journal Physics D: Applied Physics, 2016, 49, 425005.	1.3	0
349	Spatial mobility fluctuation induced giant linear magnetoresistance in multilayered graphene foam. Physical Review B, 2016, 94, .	1.1	19
350	Growth of semiconducting single-wall carbon nanotubes with a narrow band-gap distribution. Nature Communications, 2016, 7, 11160.	5.8	75
351	Electrochemical DNA sensing strategy based on strengthening electronic conduction and a signal amplifier carrier of nanoAu/MCN composited nanomaterials for sensitive lead detection. Environmental Science: Nano, 2016, 3, 1504-1509.	2.2	52
352	Elemental superdoping of graphene and carbon nanotubes. Nature Communications, 2016, 7, 10921.	5.8	238
353	Quantitative Analysis of Temperature Dependence of Raman shift of monolayer WS2. Scientific Reports, 2016, 6, 32236.	1.6	77
354	3D Grapheneâ€Foam–Reducedâ€Grapheneâ€Oxide Hybrid Nested Hierarchical Networks for Highâ€Performan Li–S Batteries. Advanced Materials, 2016, 28, 1603-1609.	ce 11.1	497
355	Selective Breaking of Hydrogen Bonds of Layered Carbon Nitride for Visible Light Photocatalysis. Advanced Materials, 2016, 28, 6471-6477.	11.1	507
356	3D Interconnected Electrode Materials with Ultrahigh Areal Sulfur Loading for Li–S Batteries. Advanced Materials, 2016, 28, 3374-3382.	11.1	488
357	Armoring Graphene Cathodes for Highâ€Rate and Longâ€Life Lithium Ion Supercapacitors. Advanced Energy Materials, 2016, 6, 1502064.	10.2	83
358	Electrochemical stability of graphene cathode for highâ€voltage lithium ion capacitors. Asia-Pacific Journal of Chemical Engineering, 2016, 11, 407-414.	0.8	3
359	Unique Domain Structure of Two-Dimensional α-Mo <sub>2</sub> C Superconducting Crystals. Nano Letters, 2016, 16, 4243-4250.	4.5	101
360	Enhanced Photocatalytic H <sub>2</sub> Production in Core–Shell Engineered Rutile TiO <sub>2</sub> . Advanced Materials, 2016, 28, 5850-5856.	11.1	183

#	Article	IF	CITATIONS
361	High Reversible Lithium Storage Capacity and Structural Changes of Fe <sub>2</sub> O <sub>3</sub> Nanoparticles Confined inside Carbon Nanotubes. Advanced Energy Materials, 2016, 6, 1501755.	10.2	109
362	A flexible cotton-derived carbon sponge for high-performance capacitive deionization. Carbon, 2016, 101, 1-8.	5.4	100
363	Tantalum (oxy)nitride based photoanodes for solar-driven water oxidation. Journal of Materials Chemistry A, 2016, 4, 2783-2800.	5.2	120
364	The smart era of electrochemical energy storage devices. Energy Storage Materials, 2016, 3, 66-68.	9.5	33
365	Scalable residue-free graphene for surface-enhanced Raman scattering. Carbon, 2016, 98, 567-571.	5.4	16
366	Epitaxial growth of single-wall carbon nanotubes. Carbon, 2016, 102, 181-197.	5.4	32
367	Efficient adsorption of organic dyes on a flexible single-wall carbon nanotube film. Journal of Materials Chemistry A, 2016, 4, 1191-1194.	5.2	48
368	Sensitive and selective detection of mercury ions based on papain and 2,6-pyridinedicarboxylic acid functionalized gold nanoparticles. RSC Advances, 2016, 6, 3259-3266.	1.7	33
369	Carbon materials for Li–S batteries: Functional evolution and performance improvement. Energy Storage Materials, 2016, 2, 76-106.	9.5	504
370	Graphene Distributed Amplifiers: Generating Desirable Gain for Graphene Field-Effect Transistors. Scientific Reports, 2015, 5, 17649.	1.6	10
371	Superiority of Graphene over Polymer Coatings for Prevention of Microbially Induced Corrosion. Scientific Reports, 2015, 5, 13858.	1.6	50
372	An Amorphous Carbon Nitride Photocatalyst with Greatly Extended Visibleâ€Lightâ€Responsive Range for Photocatalytic Hydrogen Generation. Advanced Materials, 2015, 27, 4572-4577.	11.1	771
373	Graphene-based integrated electrodes for flexible lithium ion batteries. 2D Materials, 2015, 2, 024004.	2.0	44
374	Scalable non-liquid-crystal spinning of locally aligned graphene fibers for high-performance wearable supercapacitors. Nano Energy, 2015, 15, 642-653.	8.2	172
375	Dispersible percolating carbon nano-electrodes for improvement of polysulfide utilization in Li–S batteries. Carbon, 2015, 93, 161-168.	5.4	20
376	Enhanced photocatalytic hydrogen generation of mesoporous rutile TiO2 single crystal with wholly exposed {111} facets. Chinese Journal of Catalysis, 2015, 36, 2103-2108.	6.9	35
377	Design and construction of a film of mesoporous single-crystal rutile TiO2 rod arrays for photoelectrochemical water oxidation. Chinese Journal of Catalysis, 2015, 36, 2171-2177.	6.9	19
378	Localized polyselenides in a graphene-coated polymer separator for high rate and ultralong life lithium–selenium batteries. Chemical Communications, 2015, 51, 3667-3670.	2.2	63

HUI-MING CHENG

#	Article	IF	CITATIONS
379	Open-pore LiFePO4/C microspheres with high volumetric energy density for lithium ion batteries. Particuology, 2015, 22, 24-29.	2.0	23
380	Switching Photocatalytic H <sub>2</sub> and O <sub>2</sub> Generation Preferences of Rutile TiO <sub>2</sub> Microspheres with Dominant Reactive Facets by Boron Doping. Journal of Physical Chemistry C, 2015, 119, 84-89.	1.5	18
381	Li–S Batteries: A Flexible Sulfurâ€Grapheneâ€Polypropylene Separator Integrated Electrode for Advanced Li–S Batteries (Adv. Mater. 4/2015). Advanced Materials, 2015, 27, 590-590.	11.1	4
382	Growth, metabolism of Phanerochaete chrysosporium and route of lignin degradation in response to cadmium stress in solid-state fermentation. Chemosphere, 2015, 138, 560-567.	4.2	30
383	Amorphization and Directional Crystallization of Metals Confined in Carbon Nanotubes Investigated by in Situ Transmission Electron Microscopy. Nano Letters, 2015, 15, 4922-4927.	4.5	12
384	Combined biological removal of methylene blue from aqueous solutions using rice straw and Phanerochaete chrysosporium. Applied Microbiology and Biotechnology, 2015, 99, 5247-5256.	1.7	44
385	Lithiation of Silicon Nanoparticles Confined in Carbon Nanotubes. ACS Nano, 2015, 9, 5063-5071.	7.3	105
386	Graphene based energy devices. Nanoscale, 2015, 7, 6881-2.	2.8	30
387	Greatly Enhanced Electronic Conduction and Lithium Storage of Faceted TiO <sub>2</sub> Crystals Supported on Metallic Substrates by Tuning Crystallographic Orientation of TiO <sub>2</sub> . Advanced Materials, 2015, 27, 3507-3512.	11.1	79
388	Long-term oxidation behavior of carbon/carbon composites with a SiC/B4C–B2O3–SiO2–Al2O3 coating at low and medium temperatures. Corrosion Science, 2015, 94, 452-458.	3.0	43
389	A selectively exposed crystal facet-engineered TiO2 thin film photoanode for the higher performance of the photoelectrochemical water splitting reaction. Energy and Environmental Science, 2015, 8, 3646-3653.	15.6	100
390	Synthesis of high quality nitrogen-doped single-wall carbon nanotubes. Science China Materials, 2015, 58, 603-610.	3.5	9
391	Double-Balanced Graphene Integrated Mixer with Outstanding Linearity. Nano Letters, 2015, 15, 6677-6682.	4.5	37
392	Synthesis and Application of Modified Zero-Valent Iron Nanoparticles for Removal of Hexavalent Chromium from Wastewater. Water, Air, and Soil Pollution, 2015, 226, 1.	1.1	42
393	A nitrogen-doped mesoporous carbon containing an embedded network of carbon nanotubes as a highly efficient catalyst for the oxygen reduction reaction. Nanoscale, 2015, 7, 19201-19206.	2.8	55
394	Direct writing of graphene patterns and devices on graphene oxide films by inkjet reduction. Nano Research, 2015, 8, 3954-3962.	5.8	37
395	Metal/Oxide Interface Nanostructures Generated by Surface Segregation for Electrocatalysis. Nano Letters, 2015, 15, 7704-7710.	4.5	233
396	Large-area synthesis of high-quality and uniform monolayer WS2 on reusable Au foils. Nature Communications, 2015, 6, 8569.	5.8	336

HUI-MING CHENG

#	Article	IF	CITATIONS
397	Large-area high-quality 2D ultrathin Mo2C superconducting crystals. Nature Materials, 2015, 14, 1135-1141.	13.3	1,045
398	A smart self-regenerative lithium ion supercapacitor with a real-time safety monitor. Energy Storage Materials, 2015, 1, 146-151.	9.5	28
399	An integrated composite with a porous Cf/C-ZrB2-SiC core between two compact outer layers of Cf/C-ZrB2-SiC and Cf/C-SiC. Journal of the European Ceramic Society, 2015, 35, 1113-1117.	2.8	27
400	A graphene foam electrode with high sulfur loading for flexible and high energy Li-S batteries. Nano Energy, 2015, 11, 356-365.	8.2	526
401	A Flexible Sulfurâ€Grapheneâ€Polypropylene Separator Integrated Electrode for Advanced Li–S Batteries. Advanced Materials, 2015, 27, 641-647.	11.1	545
402	Ultrafast linear dichroism-like absorption dynamics in graphene grown by chemical vapor deposition. Journal of Applied Physics, 2014, 115, .	1.1	5
403	Increasing the Visible Light Absorption of Graphitic Carbon Nitride (Melon) Photocatalysts by Homogeneous Selfâ€Modification with Nitrogen Vacancies. Advanced Materials, 2014, 26, 8046-8052.	11.1	658
404	Repeated Growth–Etching–Regrowth for Large-Area Defect-Free Single-Crystal Graphene by Chemical Vapor Deposition. ACS Nano, 2014, 8, 12806-12813.	7.3	100
405	Direct Observation of Atomic Dynamics and Silicon Doping at a Topological Defect in Graphene. Angewandte Chemie - International Edition, 2014, 53, 8908-8912.	7.2	37
406	Lithium Storage Characteristics and Possible Applications of Graphene Materials. Acta Chimica Sinica, 2014, 72, 333.	0.5	9
407	Recent advances in graphene-based planar micro-supercapacitors for on-chip energy storage. National Science Review, 2014, 1, 277-292.	4.6	298
408	De-bundling of single-wall carbon nanotubes induced by an electric field during arc discharge synthesis. Carbon, 2014, 74, 370-373.	5.4	13
409	Progress in flexible lithium batteries and future prospects. Energy and Environmental Science, 2014, 7, 1307-1338.	15.6	1,312
410	A Graphene–Pureâ€Sulfur Sandwich Structure for Ultrafast, Longâ€Life Lithium–Sulfur Batteries. Advanced Materials, 2014, 26, 625-631.	11.1	908
411	25th Anniversary Article: Carbon Nanotube―and Grapheneâ€Based Transparent Conductive Films for Optoelectronic Devices. Advanced Materials, 2014, 26, 1958-1991.	11.1	350
412	Monolithic Fe2O3/graphene hybrid for highly efficient lithium storage and arsenic removal. Carbon, 2014, 67, 500-507.	5.4	137
413	Honeycomb-like single-wall carbon nanotube networks. Journal of Materials Chemistry A, 2014, 2, 3308-3311.	5.2	2
414	Ablation and mechanical behavior of a sandwich-structured composite with an inner layer of Cf/SiC between two outer layers of Cf/SiC–ZrB2–ZrC. Corrosion Science, 2014, 80, 154-163.	3.0	52

#	Article	IF	CITATIONS
415	Photocatalysis: Constructing a Metallic/Semiconducting TaB2/Ta2O5Core/Shell Heterostructure for Photocatalytic Hydrogen Evolution (Adv. Energy Mater. 12/2014). Advanced Energy Materials, 2014, 4, n/a-n/a.	10.2	0
416	Combined removal of di(2-ethylhexyl)phthalate (DEHP) and Pb( <scp>ii</scp> ) by using a cutinase loaded nanoporous gold-polyethyleneimine adsorbent. RSC Advances, 2014, 4, 55511-55518.	1.7	47
417	Double-wall carbon nanotube transparent conductive films with excellent performance. Journal of Materials Chemistry A, 2014, 2, 1159-1164.	5.2	42
418	Selective deposition of redox co-catalyst(s) to improve the photocatalytic activity of single-domain ferroelectric PbTiO <sub>3</sub> nanoplates. Chemical Communications, 2014, 50, 10416.	2.2	100
419	Growth of metal-catalyst-free nitrogen-doped metallic single-wall carbon nanotubes. Nanoscale, 2014, 6, 12065-12070.	2.8	21
420	Structural Changes in Iron Oxide and Gold Catalysts during Nucleation of Carbon Nanotubes Studied by <i>In Situ</i> Transmission Electron Microscopy. ACS Nano, 2014, 8, 292-301.	7.3	52
421	In Situ TEM Observations on the Sulfur-Assisted Catalytic Growth of Single-Wall Carbon Nanotubes. Journal of Physical Chemistry Letters, 2014, 5, 1427-1432.	2.1	26
422	Visualizing the roles of graphene for excellent lithium storage. Journal of Materials Chemistry A, 2014, 2, 17808-17814.	5.2	48
423	CdS–mesoporous ZnS core–shell particles for efficient and stable photocatalytic hydrogen evolution under visible light. Energy and Environmental Science, 2014, 7, 1895.	15.6	379
424	The global growth of graphene. Nature Nanotechnology, 2014, 9, 726-730.	15.6	391
425	Switching the selectivity of the photoreduction reaction of carbon dioxide by controlling the band structure of a g-C <sub>3</sub> N <sub>4</sub> photocatalyst. Chemical Communications, 2014, 50, 10837.	2.2	192
426	An aqueous dissolved polysulfide cathode for lithium–sulfur batteries. Energy and Environmental Science, 2014, 7, 3307-3312.	15.6	131
427	Preparation of Metallic Single-Wall Carbon Nanotubes by Selective Etching. ACS Nano, 2014, 8, 7156-7162.	7.3	81
428	Titanium Dioxide Crystals with Tailored Facets. Chemical Reviews, 2014, 114, 9559-9612.	23.0	922
429	Batteries: A Graphene–Pureâ€Sulfur Sandwich Structure for Ultrafast, Longâ€Life Lithium–Sulfur Batteries (Adv. Mater. 4/2014). Advanced Materials, 2014, 26, 664-664.	11.1	21
430	One-Pot Synthesis of Metal–Carbon Nanotubes Network Hybrids as Highly Efficient Catalysts for Oxygen Evolution Reaction of Water Splitting. ACS Applied Materials & Interfaces, 2014, 6, 10089-10098.	4.0	40
431	Fabrication of a large-area, flexible and color-neutral single-wall carbon nanotube:sodium dodecylbenzene sulfonate/poly-(3,4-ethylenedioxythiophene):poly(4-styrenesulfonate) transparent conductive film having a new conduction mechanism. Carbon, 2014, 80, 112-119.	5.4	3
432	Constructing a Metallic/Semiconducting TaB <sub>2</sub> /Ta <sub>2</sub> O <sub>5</sub> Core/Shell Heterostructure for Photocatalytic Hydrogen Evolution. Advanced Energy Materials, 2014, 4, 1400057.	10.2	44

#	Article	IF	CITATIONS
433	A nonstoichiometric SnO2â <sup>~</sup> î <sup>~</sup> nanocrystal-based counter electrode for remarkably improving the performance of dye-sensitized solar cells. Chemical Communications, 2014, 50, 7020.	2.2	41
434	Diversity of ultrafast hot-carrier-induced dynamics and striking sub-femtosecond hot-carrier scattering times in graphene. Carbon, 2014, 72, 402-409.	5.4	14
435	Co3O4 mesoporous nanostructures@graphene membrane as an integrated anode for long-life lithium-ion batteries. Journal of Power Sources, 2014, 255, 52-58.	4.0	98
436	TiO2/graphene sandwich paper as an anisotropic electrode for high rate lithium ion batteries. Nanoscale, 2013, 5, 7780.	2.8	63
437	Crystallinity-dependent substitutional nitrogen doping in ZnO and its improved visible light photocatalytic activity. Journal of Colloid and Interface Science, 2013, 400, 18-23.	5.0	61
438	High-Quality, Highly Concentrated Semiconducting Single-Wall Carbon Nanotubes for Use in Field Effect Transistors and Biosensors. ACS Nano, 2013, 7, 6831-6839.	7.3	101
439	Edge-controlled growth and kinetics of single-crystal graphene domains by chemical vapor deposition. Proceedings of the National Academy of Sciences of the United States of America, 2013, 110, 20386-20391.	3.3	213
440	Reduced graphene oxide with a highly restored π-conjugated structure for inkjet printing and its use in all-carbon transistors. Nano Research, 2013, 6, 842-852.	5.8	68
441	The examination of graphene oxide for rechargeable lithium storage as a novel cathode material. Journal of Materials Chemistry A, 2013, 1, 3607.	5.2	73
442	Synthesis of mesoporous single crystal rutile TiO2 with improved photocatalytic and photocetalytic and photoelectrochemical activities. Chemical Communications, 2013, 49, 11770.	2.2	55
443	Graphene Foams: Superhydrophobic Graphene Foams (Small 1/2013). Small, 2013, 9, 2-2.	5.2	7
444	Patterning flexible single-walled carbon nanotube thin films by an ozone gas exposure method. Carbon, 2013, 53, 4-10.	5.4	23
445	Lightweight and Flexible Graphene Foam Composites for Highâ€Performance Electromagnetic Interference Shielding. Advanced Materials, 2013, 25, 1296-1300.	11.1	1,703
446	Effects of oxygen vacancies on the electrochemical performance of tin oxide. Journal of Materials Chemistry A, 2013, 1, 1536-1539.	5.2	125
447	Nanosize SnO2 confined in the porous shells of carbon cages for kinetically efficient and long-term lithium storage. Nanoscale, 2013, 5, 1576.	2.8	70
448	Growth of double-walled carbon nanotubes from silicon oxide nanoparticles. Carbon, 2013, 56, 167-172.	5.4	18
449	Correlation between topographic structures and local field emission characteristics of graphene-sheet films. Carbon, 2013, 61, 507-514.	5.4	18
450	Growth of tadpole-like carbon nanotubes from TiO2 nanoparticles. Carbon, 2013, 55, 253-259.	5.4	7

#	Article	IF	CITATIONS
451	Controlled Electrochemical Charge Injection to Maximize the Energy Density of Supercapacitors. Angewandte Chemie - International Edition, 2013, 52, 3722-3725.	7.2	160
452	A Review of Carbon Nanotube―and Grapheneâ€Based Flexible Thinâ€Film Transistors. Small, 2013, 9, 1188-1205.	5.2	268
453	Carbon nanotubes: controlled growth and application. Materials Today, 2013, 16, 19-28.	8.3	84
454	Visibleâ€Lightâ€Active Elemental Photocatalysts. ChemPhysChem, 2013, 14, 885-892.	1.0	93
455	Template-free synthesis of Ta3N5 nanorod arrays for efficient photoelectrochemical water splitting. Chemical Communications, 2013, 49, 3019.	2.2	115
456	Chiralityâ€Dependent Reactivity of Individual Singleâ€Walled Carbon Nanotubes. Small, 2013, 9, 1379-1386.	5.2	41
457	Tuning the Electrical and Optical Properties of Graphene by Ozone Treatment for Patterning Monolithic Transparent Electrodes. ACS Nano, 2013, 7, 4233-4241.	7.3	84
458	Self-assembled CdS/Au/ZnO heterostructure induced by surface polar charges for efficient photocatalytic hydrogen evolution. Journal of Materials Chemistry A, 2013, 1, 2773.	5.2	294
459	Visibleâ€Lightâ€Responsive βâ€Rhombohedral Boron Photocatalysts. Angewandte Chemie - International Edition, 2013, 52, 6242-6245.	7.2	99
460	A Self‧tanding and Flexible Electrode of Li <sub>4</sub> Ti <sub>5</sub> O <sub>12</sub> Nanosheets with a Nâ€Doped Carbon Coating for High Rate Lithium Ion Batteries. Advanced Functional Materials, 2013, 23, 5429-5435.	7.8	128
461	High-rate lithium storage of anatase TiO2 crystals doped with both nitrogen and sulfur. Chemical Communications, 2013, 49, 3461.	2.2	84
462	When two is better than one. Nature, 2013, 497, 448-449.	13.7	34
463	Nonstoichiometric rutile TiO2 photoelectrodes for improved photoelectrochemical water splitting. Chemical Communications, 2013, 49, 6191.	2.2	56
464	Carbon–sulfur composites for Li–S batteries: status and prospects. Journal of Materials Chemistry A, 2013, 1, 9382.	5.2	757
465	Repeated and Controlled Growth of Monolayer, Bilayer and Few-Layer Hexagonal Boron Nitride on Pt Foils. ACS Nano, 2013, 7, 5199-5206.	7.3	206
466	Fibrous Hybrid of Graphene and Sulfur Nanocrystals for High-Performance Lithium–Sulfur Batteries. ACS Nano, 2013, 7, 5367-5375.	7.3	722
467	Superhydrophobic Graphene Foams. Small, 2013, 9, 75-80.	5.2	183
468	Interstitial-boron solution strengthened WB3+ <i>x</i> . Applied Physics Letters, 2013, 103, .	1.5	72

#	Article	IF	CITATIONS
469	Nano-carbon Conductive Filmsâ $\in$ "Fabrication, Processing and Devices. , 2013, , .		0
470	A microporous–mesoporous carbon with graphitic structure for a high-rate stable sulfur cathode in carbonate solvent-based Li–S batteries. Physical Chemistry Chemical Physics, 2012, 14, 8703.	1.3	273
471	A graphene field-effect capacitor sensor in electrolyte. Applied Physics Letters, 2012, 101, .	1.5	28
472	Progress of graphene growth on copper by chemical vapor deposition: Growth behavior and controlled synthesis. Science Bulletin, 2012, 57, 2995-2999.	1.7	15
473	The doping of reduced graphene oxide with nitrogen and its effect on the quenching of the material's photoluminescence. Carbon, 2012, 50, 5286-5291.	5.4	62
474	Wall-number selective growth of vertically aligned carbon nanotubes from FePt catalysts: a comparative study with Fe catalysts. Journal of Materials Chemistry, 2012, 22, 14149.	6.7	9
475	High temperature selective growth of single-walled carbon nanotubes with a narrow chirality distribution from a CoPt bimetallic catalyst. Chemical Communications, 2012, 48, 2409.	2.2	75
476	A nanosized Fe2O3 decorated single-walled carbon nanotube membrane as a high-performance flexible anode for lithium ion batteries. Journal of Materials Chemistry, 2012, 22, 17942.	6.7	153
477	Tunable Band Gaps and p-Type Transport Properties of Boron-Doped Graphenes by Controllable Ion Doping Using Reactive Microwave Plasma. ACS Nano, 2012, 6, 1970-1978.	7.3	244
478	Quenching of fluorescence of reduced graphene oxide by nitrogen-doping. Applied Physics Letters, 2012, 100, 233112.	1.5	41
479	Hollow Anatase TiO <sub>2</sub> Single Crystals and Mesocrystals with Dominant {101} Facets for Improved Photocatalysis Activity and Tuned Reaction Preference. ACS Catalysis, 2012, 2, 1854-1859.	5.5	172
480	Flexible graphene-based lithium ion batteries with ultrafast charge and discharge rates. Proceedings of the United States of America, 2012, 109, 17360-17365.	3.3	728
481	Graphene/metal oxide composite electrode materials for energy storage. Nano Energy, 2012, 1, 107-131.	8.2	1,669
482	Boron oxynitride nanoclusters on tungsten trioxide as a metal-free cocatalyst for photocatalytic oxygen evolution from water splitting. Nanoscale, 2012, 4, 1267.	2.8	52
483	Oxygen Deficient Li <sub>4</sub> Ti <sub>5</sub> O <sub>12</sub> for Highâ€rate Lithium Storage. Journal of the Chinese Chemical Society, 2012, 59, 1201-1205.	0.8	9
484	Enrichment of Semiconducting Single-Walled Carbon Nanotubes by Carbothermic Reaction for Use in All-Nanotube Field Effect Transistors. ACS Nano, 2012, 6, 9657-9661.	7.3	27
485	Oxygen Bridges between NiO Nanosheets and Graphene for Improvement of Lithium Storage. ACS Nano, 2012, 6, 3214-3223.	7.3	977
486	A red anatase TiO2 photocatalyst for solar energy conversion. Energy and Environmental Science, 2012, 5, 9603.	15.6	379

#	Article	IF	CITATIONS
487	Synthesis and upconversion luminescence of N-doped graphene quantum dots. Applied Physics Letters, 2012, 101, .	1.5	173
488	Heteroepitaxial Growth of Single-Walled Carbon Nanotubes from Boron Nitride. Scientific Reports, 2012, 2, 971.	1.6	16
489	Crystal facet-dependent photocatalytic oxidation and reduction reactivity of monoclinic WO3 for solar energy conversion. Journal of Materials Chemistry, 2012, 22, 6746.	6.7	356
490	Graphene sponge for efficient and repeatable adsorption and desorption of water contaminations. Journal of Materials Chemistry, 2012, 22, 20197.	6.7	478
491	A flexible nanostructured sulphur–carbon nanotube cathode with high rate performance for Li-S batteries. Energy and Environmental Science, 2012, 5, 8901.	15.6	468
492	α-Sulfur Crystals as a Visible-Light-Active Photocatalyst. Journal of the American Chemical Society, 2012, 134, 9070-9073.	6.6	422
493	A LiF Nanoparticleâ€Modified Graphene Electrode for Highâ€Power and Highâ€Energy Lithium Ion Batteries. Advanced Functional Materials, 2012, 22, 3290-3297.	7.8	70
494	The Fabrication, Properties, and Uses of Graphene/Polymer Composites. Macromolecular Chemistry and Physics, 2012, 213, 1060-1077.	1.1	537
495	Nitrogen Vacancy-Promoted Photocatalytic Activity of Graphitic Carbon Nitride. Journal of Physical Chemistry C, 2012, 116, 11013-11018.	1.5	570
496	Hollow carbon cage with nanocapsules of graphitic shell/nickel core as an anode material for high rate lithium ion batteries. Journal of Materials Chemistry, 2012, 22, 11252.	6.7	69
497	Heteroatomâ€Modulated Switching of Photocatalytic Hydrogen and Oxygen Evolution Preferences of Anatase TiO <sub>2</sub> Microspheres. Advanced Functional Materials, 2012, 22, 3233-3238.	7.8	128
498	Grapheneâ€Like Carbon Nitride Nanosheets for Improved Photocatalytic Activities. Advanced Functional Materials, 2012, 22, 4763-4770.	7.8	3,009
499	Nitrogenâ€Doped Carbon Monolith for Alkaline Supercapacitors and Understanding Nitrogenâ€Induced Redox Transitions. Chemistry - A European Journal, 2012, 18, 5345-5351.	1.7	358
500	Repeated growth and bubbling transfer of graphene with millimetre-size single-crystal grains using platinum. Nature Communications, 2012, 3, 699.	5.8	985
501	A film of rutile TiO2 pillars with well-developed facets on an α-Ti substrate as a photoelectrode for improved water splitting. Nanoscale, 2012, 4, 3871.	2.8	29
502	Template synthesis of ultra-thin and short carbon nanotubes with two open ends. Journal of Materials Chemistry, 2012, 22, 15221.	6.7	16
503	The reduction of graphene oxide. Carbon, 2012, 50, 3210-3228.	5.4	4,247
504	ZnO–CdS@Cd Heterostructure for Effective Photocatalytic Hydrogen Generation. Advanced Energy Materials, 2012, 2, 42-46.	10.2	191

#	Article	IF	CITATIONS
505	Photocatalysis: ZnO-CdS@Cd Heterostructure for Effective Photocatalytic Hydrogen Generation (Adv. Energy Mater. 1/2012). Advanced Energy Materials, 2012, 2, 2-2.	10.2	1
506	Carbon nanotubes prepared by anodic aluminum oxide template method. Science Bulletin, 2012, 57, 187-204.	1.7	35
507	Controlled Shaping TiO2 for Efficient Photocatalysis. , 2012, , 43-72.		0
508	Achieving maximum photo-oxidation reactivity of Cs0.68Ti1.83O4â^'xNx photocatalysts through valence band fine-tuning. Catalysis Science and Technology, 2011, 1, 222.	2.1	32
509	Contamination-free and damage-free patterning of single-walled carbon nanotube transparent conductive films on flexible substrates. Nanoscale, 2011, 3, 4571.	2.8	9
510	Polar interface-induced improvement in high photocatalytic hydrogen evolution over ZnO–CdS heterostructures. Energy and Environmental Science, 2011, 4, 3976.	15.6	147
511	Bandgap narrowing of titanium oxide nanosheets: homogeneous doping of molecular iodine for improved photoreactivity. Journal of Materials Chemistry, 2011, 21, 14672.	6.7	28
512	Synthesis of anatase TiO2 rods with dominant reactive {010} facets for the photoreduction of CO2 to CH4 and use in dye-sensitized solar cells. Chemical Communications, 2011, 47, 8361.	2.2	196
513	TiO <sub>2</sub> films with oriented anatase {001} facets and their photoelectrochemical behavior as CdS nanoparticle sensitized photoanodes. Journal of Materials Chemistry, 2011, 21, 869-873.	6.7	107
514	Bulk Synthesis of Large Diameter Semiconducting Single-Walled Carbon Nanotubes by Oxygen-Assisted Floating Catalyst Chemical Vapor Deposition. Journal of the American Chemical Society, 2011, 133, 5232-5235.	6.6	134
515	Anatase TiO <sub>2</sub> Crystal Facet Growth: Mechanistic Role of Hydrofluoric Acid and Photoelectrocatalytic Activity. ACS Applied Materials & amp; Interfaces, 2011, 3, 2472-2478.	4.0	108
516	Tunable p-Type Conductivity and Transport Properties of AlN Nanowires <i>via</i> Mg Doping. ACS Nano, 2011, 5, 3591-3598.	7.3	47
517	Synthesis and field emission property of carbon nanotubes with sharp tips. New Carbon Materials, 2011, 26, 52-56.	2.9	21
518	The effect of carbon particle morphology on the electrochemical properties of nanocarbon/polyaniline composites in supercapacitors. New Carbon Materials, 2011, 26, 180-186.	2.9	34
519	A sandwich structure of graphene and nickel oxide with excellent supercapacitive performance. Journal of Materials Chemistry, 2011, 21, 9014.	6.7	125
520	Doped Graphene Sheets As Anode Materials with Superhigh Rate and Large Capacity for Lithium Ion Batteries. ACS Nano, 2011, 5, 5463-5471.	7.3	1,904
521	Crystal facet engineering of semiconductor photocatalysts: motivations, advances and unique properties. Chemical Communications, 2011, 47, 6763.	2.2	867
522	Three-dimensional flexible and conductive interconnected graphene networks grown by chemical vapour deposition. Nature Materials, 2011, 10, 424-428.	13.3	3,493

HUI-MING CHENG

#	Article	IF	CITATIONS
523	Nanosized Li4Ti5O12/graphene hybrid materials with low polarization for high rate lithium ion batteries. Journal of Power Sources, 2011, 196, 8610-8617.	4.0	306
524	High Sensitivity Gas Detection Using a Macroscopic Three-Dimensional Graphene Foam Network. Scientific Reports, 2011, 1, 166.	1.6	503
525	Importance of Oxygen in the Metal-Free Catalytic Growth of Single-Walled Carbon Nanotubes from SiO <sub><i>x</i></sub> by a Vaporâ^`Solidâ^`Solid Mechanism. Journal of the American Chemical Society, 2011, 133, 197-199.	6.6	116
526	Additiveâ€Free Dispersion of Singleâ€Walled Carbon Nanotubes and Its Application for Transparent Conductive Films. Advanced Functional Materials, 2011, 21, 2330-2337.	7.8	51
527	Battery Performance and Photocatalytic Activity of Mesoporous Anatase TiO <sub>2</sub> Nanospheres/Graphene Composites by Templateâ€Free Selfâ€Assembly. Advanced Functional Materials, 2011, 21, 1717-1722.	7.8	601
528	Vertically Aligned Carbon Nanotubes Grown on Graphene Paper as Electrodes in Lithiumâ€lon Batteries and Dyeâ€Sensitized Solar Cells. Advanced Energy Materials, 2011, 1, 486-490.	10.2	309
529	Graphene–Cellulose Paper Flexible Supercapacitors. Advanced Energy Materials, 2011, 1, 917-922.	10.2	831
530	On the True Photoreactivity Order of {001}, {010}, and {101} Facets of Anatase TiO <sub>2</sub> Crystals. Angewandte Chemie - International Edition, 2011, 50, 2133-2137.	7.2	1,106
531	Facile Fabrication of Anatase TiO <sub>2</sub> Microspheres on Solid Substrates and Surface Crystal Facet Transformation from {001} to {101}. Chemistry - A European Journal, 2011, 17, 5949-5957.	1.7	70
532	Fermi level dependent optical transition energy in metallic single-walled carbon nanotubes. Carbon, 2011, 49, 4774-4780.	5.4	14
533	Edge phonon state of mono- and few-layer graphene nanoribbons observed by surface and interference co-enhanced Raman spectroscopy. Physical Review B, 2010, 81, .	1.1	77
534	Highly efficient H <sub>2</sub> evolution over ZnO-ZnS-CdS heterostructures from an aqueous solution containing SO <sub>3</sub> <sup>2-</sup> and S <sup>2-</sup> ions. Journal of Materials Research, 2010, 25, 39-44.	1.2	37
535	Efficient synthesis of graphene nanoribbons sonochemically cut from graphene sheets. Nano Research, 2010, 3, 16-22.	5.8	143
536	Anchoring Hydrous RuO <sub>2</sub> on Graphene Sheets for Highâ€Performance Electrochemical Capacitors. Advanced Functional Materials, 2010, 20, 3595-3602.	7.8	1,122
537	Advanced Materials for Energy Storage. Advanced Materials, 2010, 22, E28-62.	11.1	4,168
538	ZnS Branched Architectures as Optoelectronic Devices and Field Emitters. Advanced Materials, 2010, 22, 2376-2380.	11.1	96
539	Sulfur doped anatase TiO2 single crystals with a high percentage of {0 0 1} facets. Journal of Colloid and Interface Science, 2010, 349, 477-483.	5.0	112
540	Hydrogen generation from sodium borohydride solution using a ruthenium supported on graphite catalyst. International Journal of Hydrogen Energy, 2010, 35, 3023-3028.	3.8	167

#	Article	IF	CITATIONS
541	Hydrogen sorption kinetics of MgH2 catalyzed with titanium compounds. International Journal of Hydrogen Energy, 2010, 35, 3046-3050.	3.8	80
542	Stable photocatalytic hydrogen evolution from water over ZnO–CdS core–shell nanorods. International Journal of Hydrogen Energy, 2010, 35, 8199-8205.	3.8	229
543	Hydrogen storage in carbon nanotubes revisited. Carbon, 2010, 48, 452-455.	5.4	190
544	Selective removal of metallic single-walled carbon nanotubes by combined in situ and post-synthesis oxidation. Carbon, 2010, 48, 2941-2947.	5.4	50
545	Bulk growth of mono- to few-layer graphene on nickel particles by chemical vapor deposition from methane. Carbon, 2010, 48, 3543-3550.	5.4	96
546	Increasing the electrical conductivity of carbon nanotube/polymer composites by using weak nanotube–polymer interactions. Carbon, 2010, 48, 3551-3558.	5.4	103
547	Direct reduction of graphene oxide films into highly conductive and flexible graphene films by hydrohalic acids. Carbon, 2010, 48, 4466-4474.	5.4	1,459
548	Synthesis of single-walled carbon nanotubes, their ropes and books. Comptes Rendus Physique, 2010, 11, 349-354.	0.3	10
549	Fluorographene: A Twoâ€Dimensional Counterpart of Teflon. Small, 2010, 6, 2877-2884.	5.2	1,146
550	Carbon nanotube-clamped metal atomic chain. Proceedings of the National Academy of Sciences of the United States of America, 2010, 107, 9055-9059.	3.3	36
551	Zinc sulfide nanowire arrays on silicon wafers for field emitters. Nanotechnology, 2010, 21, 065701.	1.3	19
552	Triangle defect states of hexagonal boron nitride atomic layer: Density functional theory calculations. Physical Review B, 2010, 81, .	1.1	60
553	Effects of carbon on hydrogen storage performances of hydrides. Journal of Materials Chemistry, 2010, 20, 5390.	6.7	116
554	Efficient growth of high-quality graphene films on Cu foils by ambient pressure chemical vapor deposition. Applied Physics Letters, 2010, 97, .	1.5	176
555	Free-Standing Highly Conductive Transparent Ultrathin Single-Walled Carbon Nanotube Films. Journal of the American Chemical Society, 2010, 132, 16581-16586.	6.6	83
556	Efficient Preparation of Large-Area Graphene Oxide Sheets for Transparent Conductive Films. ACS Nano, 2010, 4, 5245-5252.	7.3	869
557	Development of graphene-based materials for energy storage. , 2010, , .		3
558	Titania-based photocatalysts—crystal growth, doping and heterostructuring. Journal of Materials Chemistry, 2010, 20, 831-843.	6.7	1,028

#	Article	IF	CITATIONS
559	Nanosized anatase TiO2 single crystals for enhanced photocatalytic activity. Chemical Communications, 2010, 46, 755-757.	2.2	403
560	Incorporation of Graphenes in Nanostructured TiO <sub>2</sub> Films <i>via</i> Molecular Grafting for Dye-Sensitized Solar Cell Application. ACS Nano, 2010, 4, 3482-3488.	7.3	471
561	Graphene Anchored with Co <sub>3</sub> O <sub>4</sub> Nanoparticles as Anode of Lithium Ion Batteries with Enhanced Reversible Capacity and Cyclic Performance. ACS Nano, 2010, 4, 3187-3194.	7.3	2,358
562	Graphene-Wrapped Fe <sub>3</sub> O <sub>4</sub> Anode Material with Improved Reversible Capacity and Cyclic Stability for Lithium Ion Batteries. Chemistry of Materials, 2010, 22, 5306-5313.	3.2	1,773
563	Preparation and electrochemical property of Fe2O3 nanoparticles-filled carbon nanotubes. Chemical Communications, 2010, 46, 8576.	2.2	116
564	High-Energy MnO <sub>2</sub> Nanowire/Graphene and Graphene Asymmetric Electrochemical Capacitors. ACS Nano, 2010, 4, 5835-5842.	7.3	1,448
565	Unique Electronic Structure Induced High Photoreactivity of Sulfur-Doped Graphitic C <sub>3</sub> N <sub>4</sub> . Journal of the American Chemical Society, 2010, 132, 11642-11648.	6.6	1,856
566	Long wavelength emissions of periodic yard-glass shaped boron nitride nanotubes. Applied Physics Letters, 2009, 94, 023105.	1.5	18
567	Thermal properties of nanocrystalline Al composites reinforced by AlN nanoparticles. Journal of Materials Research, 2009, 24, 24-31.	1.2	22
568	Effect of Li <sub>3</sub> N additive on the hydrogen storage properties of Li-Mg-N-H system. Journal of Materials Research, 2009, 24, 1936-1942.	1.2	12
569	Lithium atalyzed Dehydrogenation of Ammonia Borane within Mesoporous Carbon Framework for Chemical Hydrogen Storage. Advanced Functional Materials, 2009, 19, 265-271.	7.8	156
570	Field Emission and Cathodoluminescence of ZnS Hexagonal Pyramids of Zinc Blende Structured Single Crystals. Advanced Functional Materials, 2009, 19, 484-490.	7.8	47
571	Field Emission of Singleâ€Layer Graphene Films Prepared by Electrophoretic Deposition. Advanced Materials, 2009, 21, 1756-1760.	11.1	624
572	Selfâ€Assembled Freeâ€Standing Graphite Oxide Membrane. Advanced Materials, 2009, 21, 3007-3011.	11.1	868
573	A Comparative Study of the Structural, Electronic, and Vibrational Properties of NH <sub>3</sub> BH <sub>3</sub> and LiNH <sub>2</sub> BH <sub>3</sub> : Theory and Experiment. ChemPhysChem, 2009, 10, 1825-1833.	1.0	38
574	A General Single‣ource Route for the Preparation of Hollow Nanoporous Metal Oxide Structures. Angewandte Chemie - International Edition, 2009, 48, 7048-7051.	7.2	106
575	3D Aperiodic Hierarchical Porous Graphitic Carbon Material for Highâ€Rate Electrochemical Capacitive Energy Storage. Angewandte Chemie - International Edition, 2009, 48, 1525-1525.	7.2	55
576	Effect of carbonization atmosphere on the structure changes of PAN carbon membranes. Journal of Porous Materials, 2009, 16, 197-203.	1.3	42

#	Article	IF	CITATIONS
577	Electrochemical interfacial capacitance in multilayer graphene sheets: Dependence on number of stacking layers. Electrochemistry Communications, 2009, 11, 1729-1732.	2.3	160
578	Hydrogen adsorption behavior of graphene above critical temperature. International Journal of Hydrogen Energy, 2009, 34, 2329-2332.	3.8	203
579	The role of crystal phase in determining photocatalytic activity of nitrogen doped TiO2. Journal of Colloid and Interface Science, 2009, 329, 331-338.	5.0	104
580	Drastically enhanced photocatalytic activity in nitrogen doped mesoporous TiO2 with abundant surface states. Journal of Colloid and Interface Science, 2009, 334, 171-175.	5.0	68
581	Efficient and stable photocatalytic H2 evolution from water splitting by (Cd0.8Zn0.2)S nanorods. Electrochemistry Communications, 2009, 11, 1174-1178.	2.3	60
582	Synthesis of high-quality graphene with a pre-determined number of layers. Carbon, 2009, 47, 493-499.	5.4	650
583	Structural evolution of carbon microcoils induced by a direct current. Carbon, 2009, 47, 670-674.	5.4	12
584	Semiconducting properties of cup-stacked carbon nanotubes. Carbon, 2009, 47, 731-736.	5.4	56
585	Enhanced photocatalytic hydrogen evolution by prolonging the lifetime of carriers in ZnO/CdS heterostructures. Chemical Communications, 2009, , 3452.	2.2	476
586	Metal-Catalyst-Free Growth of Single-Walled Carbon Nanotubes. Journal of the American Chemical Society, 2009, 131, 2082-2083.	6.6	258
587	Enhanced Photoactivity of Oxygen-Deficient Anatase TiO <sub>2</sub> Sheets with Dominant {001} Facets. Journal of Physical Chemistry C, 2009, 113, 21784-21788.	1.5	376
588	Fabrication of Graphene/Polyaniline Composite Paper <i>via In Situ</i> Anodic Electropolymerization for High-Performance Flexible Electrode. ACS Nano, 2009, 3, 1745-1752.	7.3	1,464
589	Crystallographic Tailoring of Graphene by Nonmetal SiO <sub><i>x</i></sub> Nanoparticles. Journal of the American Chemical Society, 2009, 131, 13934-13936.	6.6	68
590	Enhanced Hydrogen Storage Properties of Liâ^'Mgâ^'Nâ^'H System Prepared by Reacting Mg(NH2)2 with Li3N. Journal of Physical Chemistry C, 2009, 113, 9944-9949.	1.5	25
591	Synthesis and Photoelectrochemical Property of Urchin-like Zn/ZnO Coreâ~'Shell Structures. Journal of Physical Chemistry C, 2009, 113, 11035-11040.	1.5	73
592	Catalytically enhanced dehydrogenation of Li–Mg–N–H hydrogen storage material by transition metal nitrides. Journal of Alloys and Compounds, 2009, 468, L21-L24.	2.8	37
593	Synthesis of Graphene Sheets with High Electrical Conductivity and Good Thermal Stability by Hydrogen Arc Discharge Exfoliation. ACS Nano, 2009, 3, 411-417.	7.3	807
594	Band-to-Band Visible-Light Photon Excitation and Photoactivity Induced by Homogeneous Nitrogen Doping in Layered Titanates. Chemistry of Materials, 2009, 21, 1266-1274.	3.2	284

#	Article	IF	CITATIONS
595	Surface and Interference Coenhanced Raman Scattering of Graphene. ACS Nano, 2009, 3, 933-939.	7.3	87
596	Visible Light Responsive Nitrogen Doped Anatase TiO <sub>2</sub> Sheets with Dominant {001} Facets Derived from TiN. Journal of the American Chemical Society, 2009, 131, 12868-12869.	6.6	570
597	<i>In Situ</i> Assembly of Multi-Sheeted Buckybooks from Single-Walled Carbon Nanotubes. ACS Nano, 2009, 3, 707-713.	7.3	39
598	Titania polymorphs derived from crystalline titanium diboride. CrystEngComm, 2009, 11, 2677.	1.3	42
599	The fabrication of a carbon nanotube transparent conductive film by electrophoretic deposition and hot-pressing transfer. Nanotechnology, 2009, 20, 235707.	1.3	79
600	Efficient Promotion of Anatase TiO2 Photocatalysis via Bifunctional Surface-Terminating Tiâ^'Oâ^'Bâ^'N Structures. Journal of Physical Chemistry C, 2009, 113, 12317-12324.	1.5	115
601	Growth Velocity and Direct Length-Sorted Growth of Short Single-Walled Carbon Nanotubes by a Metal-Catalyst-Free Chemical Vapor Deposition Process. ACS Nano, 2009, 3, 3421-3430.	7.3	76
602	Synthesis of rutile–anatase core–shell structured TiO2 for photocatalysis. Journal of Materials Chemistry, 2009, 19, 6590.	6.7	112
603	Nitrogen-doped titania nanosheets towards visible light response. Chemical Communications, 2009, , 1383.	2.2	95
604	lodine doped anatase TiO2 photocatalyst with ultra-long visible light response: correlation between geometric/electronic structures and mechanisms. Journal of Materials Chemistry, 2009, 19, 2822.	6.7	127
605	Comparison of the rate capability of nanostructured amorphous and anatase TiO <sub>2</sub> for lithium insertion using anodic TiO <sub>2</sub> nanotube arrays. Nanotechnology, 2009, 20, 225701.	1.3	194
606	In situ formation and rapid decomposition of Ti(BH4)3 by mechanical milling LiBH4 with TiF3. Applied Physics Letters, 2009, 94, 044104.	1.5	44
607	Synthesis and Photoelectrochemical Behavior of Nitrogen-doped NaTaO3. Chemistry Letters, 2009, 38, 214-215.	0.7	24
608	Enhancement of Field Emission of CNTs Array by CO <sub>2</sub> -Assisted Chemical Vapor Deposition. Journal of Nanoscience and Nanotechnology, 2009, 9, 3046-3051.	0.9	6
609	Ti-Zr-O Nanotube Arrays with Controlled Morphology, Crystal Structure and Optical Properties. Journal of Nanoscience and Nanotechnology, 2009, 9, 6501-6510.	0.9	6
610	Synthesis, Purification and Opening of Short Cup-Stacked Carbon Nanotubes. Journal of Nanoscience and Nanotechnology, 2009, 9, 4554-4560.	0.9	15
611	Standard enthalpies of formation of finite-length (5, 5) single-walled carbon nanotube. Journal of Nanoparticle Research, 2008, 10, 1037-1043.	0.8	1
612	ZnO microcolumns originated from self-assembled nanorods. Journal of Materials Science, 2008, 43, 1711-1715.	1.7	7

#	Article	IF	CITATIONS
613	3D Aperiodic Hierarchical Porous Graphitic Carbon Material for Highâ€Rate Electrochemical Capacitive Energy Storage. Angewandte Chemie - International Edition, 2008, 47, 373-376.	7.2	1,747
614	Synergistic Effects of B/N Doping on the Visibleâ€Light Photocatalytic Activity of Mesoporous TiO <sub>2</sub> . Angewandte Chemie - International Edition, 2008, 47, 4516-4520.	7.2	484
615	Controllable Synthesis of Vertically Aligned pâ€₹ype GaN Nanorod Arrays on nâ€∓ype Si Substrates for Heterojunction Diodes. Advanced Functional Materials, 2008, 18, 3515-3522.	7.8	50
616	Growth, Cathodoluminescence and Field Emission of ZnS Tetrapod Treeâ€like Heterostructures. Advanced Functional Materials, 2008, 18, 3063-3069.	7.8	48
617	Aligned Titania Nanotubes as an Intercalation Anode Material for Hybrid Electrochemical Energy Storage. Advanced Functional Materials, 2008, 18, 3787-3793.	7.8	97
618	Ammonia Borane Destabilized by Lithium Hydride: An Advanced Onâ€Board Hydrogen Storage Material. Advanced Materials, 2008, 20, 2756-2759.	11.1	183
619	Amorphous cobalt–boron/nickel foam as an effective catalyst for hydrogen generation from alkaline sodium borohydride solution. Journal of Power Sources, 2008, 177, 17-23.	4.0	181
620	Hierarchical porous nickel oxide and carbon as electrode materials for asymmetric supercapacitor. Journal of Power Sources, 2008, 185, 1563-1568.	4.0	439
621	Thermodynamically tuning LiBH4 by fluorine anion doping for hydrogen storage: A density functional study. Chemical Physics Letters, 2008, 450, 318-321.	1.2	101
622	Selected absorption behavior of sulfur on single-walled carbon nanotubes by DFT. Chemical Physics Letters, 2008, 454, 305-309.	1.2	18
623	Direct synthesis of carbon nanotubes decorated with size-controllable Fe nanoparticles encapsulated by graphitic layers. Carbon, 2008, 46, 1417-1423.	5.4	57
624	Synthesis and dye separation performance of ferromagnetic hierarchical porous carbon. Carbon, 2008, 46, 1593-1599.	5.4	80
625	Synthesis of different magnetic carbon nanostructures by the pyrolysis of ferrocene at different sublimation temperatures. Carbon, 2008, 46, 1892-1902.	5.4	69
626	Purification of carbon nanotubes. Carbon, 2008, 46, 2003-2025.	5.4	660
627	Synthesis and Electrochemical Property of Boron-Doped Mesoporous Carbon in Supercapacitor. Chemistry of Materials, 2008, 20, 7195-7200.	3.2	511
628	Novel Boron Nitride Hollow Nanoribbons. ACS Nano, 2008, 2, 2183-2191.	7.3	192
629	Amorphous TiO <sub>2</sub> nanotube arrays for low-temperature oxygen sensors. Nanotechnology, 2008, 19, 405504.	1.3	178
630	Frequency response characteristic of single-walled carbon nanotubes as supercapacitor electrode material. Applied Physics Letters, 2008, 92, .	1.5	102

#	Article	IF	CITATIONS
631	Manganese-Catalyzed Surface Growth of Single-Walled Carbon Nanotubes with High Efficiency. Journal of Physical Chemistry C, 2008, 112, 19231-19235.	1.5	37
632	Diameter-Selective Growth of Single-Walled Carbon Nanotubes with High Quality by Floating Catalyst Method. ACS Nano, 2008, 2, 1722-1728.	7.3	88
633	Raman Spectroscopy on Double-Walled Carbon Nanotubes. , 2008, , 29-39.		1
634	Synthesis of Tin (II or IV) Oxide Coated Multiwall Carbon Nanotubes with Controlled Morphology. Journal of Physical Chemistry C, 2008, 112, 5790-5794.	1.5	46
635	Mesopore-Aspect-Ratio Dependence of Ion Transport in Rodtype Ordered Mesoporous Carbon. Journal of Physical Chemistry C, 2008, 112, 9950-9955.	1.5	98
636	Electron field emission of a nitrogen-doped TiO2nanotube array. Nanotechnology, 2008, 19, 025606.	1.3	127
637	Hydrogen sorption kinetics of MgH2 catalyzed with NbF5. Journal of Alloys and Compounds, 2008, 453, 138-142.	2.8	82
638	Enhanced H-storage property in Li–Co–N–H system by promoting ion migration. Journal of Alloys and Compounds, 2008, 466, L1-L4.	2.8	12
639	Vertically Aligned p-Type Single-Crystalline GaN Nanorod Arrays on n-Type Si for Heterojunction Photovoltaic Cells. Nano Letters, 2008, 8, 4191-4195.	4.5	298
640	Total Color Difference for Rapid and Accurate Identification of Graphene. ACS Nano, 2008, 2, 1625-1633.	7.3	135
641	Self-Assembly and Cathodoluminescence of Microbelts from Cu-Doped Boron Nitride Nanotubes. ACS Nano, 2008, 2, 1523-1532.	7.3	41
642	Improving the electrochemical properties of natural graphite spheres by coating with a pyrolytic carbon shell. New Carbon Materials, 2008, 23, 30-36.	2.9	14
643	Improved Reversible Dehydrogenation of Lithium Borohydride by Milling with As-Prepared Single-Walled Carbon Nanotubes. Journal of Physical Chemistry C, 2008, 112, 17023-17029.	1.5	69
644	Catalytically Enhanced Hydrogen Storage Properties of Mg(NH <sub>2</sub> ) <sub>2</sub> + 2LiH Material by Graphite-Supported Ru Nanoparticles. Journal of Physical Chemistry C, 2008, 112, 18280-18285.	1.5	42
645	Poly(vinyl chloride) (PVC) Coated Idea Revisited: Influence of Carbonization Procedures on PVC-Coated Natural Graphite as Anode Materials for Lithium Ion Batteries. Journal of Physical Chemistry C, 2008, 112, 7767-7772.	1.5	38
646	The facile synthesis of nickel silicide nanobelts and nanosheets and their application in electrochemical energy storage. Nanotechnology, 2008, 19, 165606.	1.3	31
647	<i>In situ</i> electrical measurements of polytypic silver nanowires. Nanotechnology, 2008, 19, 085711.	1.3	36
648	Probing quantum confinement of single-walled carbon nanotubes by resonant soft-x-ray emission spectroscopy. Applied Physics Letters, 2008, 93, .	1.5	12

#	Article	IF	CITATIONS
649	Pyrolytic carbon-coated silicon/Carbon Nanotube composites: promising application for Li-ion batteries. International Journal of Nanomanufacturing, 2008, 2, 4.	0.3	14
650	How long can single-walled carbon nanotube ropes last under static or dynamic fatigue?. Applied Physics Letters, 2008, 92, 083105.	1.5	10
651	Synthesis and Properties of Quasi-One-Dimensional Nitride Nanostructures. , 2008, , 149-177.		0
652	Interface Design of Carbon Nano-Materials for Energy Storage. , 2008, , 41-47.		0
653	Effect of Mn And Zr on Hydrogen Absorption in Mg-Based Nanocomposites. NATO Science for Peace and Security Series C: Environmental Security, 2008, , 497-502.	0.1	0
654	Controlled synthesis of quasi-one-dimensional boron nitride nanostructures. Journal of Materials Research, 2007, 22, 2809-2816.	1.2	17
655	ZnS nanowires and their coaxial lateral nanowire heterostructures with BN. Applied Physics Letters, 2007, 90, 103117.	1.5	32
656	Preliminary investigation on the catalytic mechanism of TiF3 additive in MgH2–TiF3 H-storage system. Journal of Materials Research, 2007, 22, 1779-1786.	1.2	14
657	Improving hydrogen sorption kinetics of MgH2 by mechanical milling with TiF3. Journal of Alloys and Compounds, 2007, 432, L1-L4.	2.8	65
658	Improved capacitance of SBA-15 templated mesoporous carbons after modification with nitric acid oxidation. New Carbon Materials, 2007, 22, 307-314.	2.9	95
659	Effects of Carbon Nanotubes on Processing Stability of Polyoxymethylene in Meltâ^'Mixing Process. Journal of Physical Chemistry C, 2007, 111, 13945-13950.	1.5	40
660	A Raman probe for selective wrapping of single-walled carbon nanotubes by DNA. Nanotechnology, 2007, 18, 405706.	1.3	27
661	Functional anion concept: effect of fluorine anion on hydrogen storage of sodium alanate. Physical Chemistry Chemical Physics, 2007, 9, 1499-1502.	1.3	83
662	Synthesis and High Thermal Stability of Double-Walled Carbon Nanotubes Using Nickel Formate Dihydrate as Catalyst Precursor. Journal of Physical Chemistry C, 2007, 111, 5006-5013.	1.5	50
663	Metallic and Carbon Nanotube-Catalyzed Coupling of Hydrogenation in Magnesium. Journal of the American Chemical Society, 2007, 129, 15650-15654.	6.6	131
664	Facile and Controlled Synthesis of 3D Nanorods-Based Urchinlike and Nanosheets-Based Flowerlike Cobalt Basic Salt Nanostructures. Journal of Physical Chemistry C, 2007, 111, 3848-3852.	1.5	88
665	Improving Hydrogen Storage Performance of NaAlH4by Novel Two-Step Milling Method. Journal of Physical Chemistry C, 2007, 111, 4879-4884.	1.5	22
666	SYNTHESIS AND PROPERTIES OF ONE-DIMENSIONAL ALUMINUM NITRIDE NANOSTRUCTURES. Nano, 2007, 02, 307-331.	0.5	11

#	Article	IF	CITATIONS
667	New Insight into the Interaction between Propylene Carbonate-Based Electrolytes and Graphite Anode Material for Lithium Ion Batteries. Journal of Physical Chemistry C, 2007, 111, 4740-4748.	1.5	37
668	Synthesis and photoluminescent property of AlN nanobelt array. Diamond and Related Materials, 2007, 16, 537-541.	1.8	48
669	Synthesis and photoluminescence of tetrapod ZnO nanostructures. Chemical Physics Letters, 2007, 434, 301-305.	1.2	64
670	A comparison between field-emission properties of three one-dimensional carbon materials. Physica B: Condensed Matter, 2007, 396, 44-48.	1.3	7
671	Swelling and mechanical behaviors of carbon nanotube/poly(vinyl alcohol) hybrid hydrogels. Materials Letters, 2007, 61, 1704-1706.	1.3	154
672	A simple and low-temperature hydrothermal route for the synthesis of tubular α-FeOOH. Materials Letters, 2007, 61, 4794-4796.	1.3	36
673	Advantage of TiF3 over TiCl3 as a dopant precursor to improve the thermodynamic property of Na3AlH6. Scripta Materialia, 2007, 56, 361-364.	2.6	31
674	Enhanced hydrogen storage properties of MgH2 co-catalyzed with NbF5 and single-walled carbon nanotubes. Scripta Materialia, 2007, 56, 765-768.	2.6	57
675	Reversible hydrogen storage in LiBH4 destabilized by milling with Al. Applied Physics A: Materials Science and Processing, 2007, 89, 963-966.	1.1	128
676	Mg-Based Nanocomposites with High Capacity and Fast Kinetics for Hydrogen Storage. Journal of Physical Chemistry B, 2006, 110, 11697-11703.	1.2	95
677	Effect of Pore Packing Defects in 2-D Ordered Mesoporous Carbons on Ionic Transport. Journal of Physical Chemistry B, 2006, 110, 8570-8575.	1.2	144
678	Double-walled carbon nanotubes synthesized using carbon black as the dot carbon source. Nanotechnology, 2006, 17, 3100-3104.	1.3	29
679	Visible Light Photocatalyst:Â Iodine-Doped Mesoporous Titania with a Bicrystalline Framework. Journal of Physical Chemistry B, 2006, 110, 20823-20828.	1.2	236
680	Evidence for, and an Understanding of, the Initial Nucleation of Carbon Nanotubes Produced by a Floating Catalyst Method. Journal of Physical Chemistry B, 2006, 110, 16941-16946.	1.2	45
681	Electron microscopy study of Ti-doped sodium aluminum hydride prepared by mechanical milling NaHâ^•Al with Ti powder. Journal of Applied Physics, 2006, 100, 034914.	1.1	18
682	Electrochemical performance of pyrolytic carbon-coated natural graphite spheres. Carbon, 2006, 44, 2212-2218.	5.4	105
683	Urchin-like nano/micro hybrid anode materials for lithium ion battery. Carbon, 2006, 44, 2778-2784.	5.4	62
684	Structure and morphology of microporous carbon membrane materials derived from poly(phthalazinone ether sulfone ketone). Microporous and Mesoporous Materials, 2006, 96, 79-83.	2.2	44

#	Article	IF	CITATIONS
685	Structure and hydrogen storage property of ball-milled LiNH2/MgH2LiNH2/MgH2 mixture. International Journal of Hydrogen Energy, 2006, 31, 1236-1240.	3.8	57
686	Raman evidence for atomic correlation between the two constituent tubes in double-walled carbon nanotubes. Physical Review B, 2006, 73, .	1.1	15
687	Pore structures of multi-walled carbon nanotubes activated by air, CO2 and KOH. Journal of Porous Materials, 2006, 13, 141-146.	1.3	51
688	The role of NH3 atmosphere in preparing nitrogen-doped TiO2 by mechanochemical reaction. Journal of Solid State Chemistry, 2006, 179, 331-335.	1.4	53
689	An environment-friendly microemulsion approach to α-FeOOH nanorods at room temperature. Materials Research Bulletin, 2006, 41, 2238-2243.	2.7	36
690	Selective Heterogeneous Nucleation and Growth of Size-Controlled Metal Nanoparticles on Carbon Nanotubes in Solution. Chemistry - A European Journal, 2006, 12, 2542-2549.	1.7	124
691	Preparation of High Purity ZnO Nanobelts by Thermal Evaporation of ZnS. Journal of Nanoscience and Nanotechnology, 2006, 6, 704-707.	0.9	20
692	Effects of Carbon Nanotubes and Metal Catalysts on Hydrogen Storage in Magnesium Nanocomposites. Journal of Nanoscience and Nanotechnology, 2006, 6, 494-498.	0.9	25
693	The Effect of Sulfur on the Structure of Carbon Nanotubes Produced by a Floating Catalyst Method. Journal of Nanoscience and Nanotechnology, 2006, 6, 1339-1345.	0.9	62
694	PLATELET BORON NITRIDE NANOWIRES. Nano, 2006, 01, 65-71.	0.5	7
695	Controlled growth of two-dimensional â€~single-crystal' hafnia networks by surface modulation. Nanotechnology, 2006, 17, 1207-1211.	1.3	4
696	A simple solution route to controlled synthesis of ZnS submicrospheres, nanosheets and nanorods. Nanotechnology, 2006, 17, 4731-4735.	1.3	34
697	Graphitization-induced microstructural changes in tetrahydrofuran-derived pyrolytic carbon spheres. Journal of Materials Research, 2006, 21, 2198-2203.	1.2	9
698	Carbon nanotubes enhanced hydrogen ab/desorption in Magnesium-based nanocomposites. , 2006, , .		1
699	Thermal characterization of single-wall carbon nanotube bundles using the self-heating 3ï‰ technique. Journal of Applied Physics, 2006, 100, 124314.	1.1	48
700	Magnetic nanocables—Silicon carbide sheathed with iron-oxide-doped amorphous silica. Applied Physics Letters, 2006, 88, 043105.	1.5	9
701	Shaping different carbon nano- and submicro-structures by alcohol chemical vapor deposition. Journal of Materials Research, 2006, 21, 2504-2509.	1.2	1
702	Simple approach to estimating the van der Waals interaction between carbon nanotubes. Physical Review B, 2006, 73, .	1.1	27

#	Article	IF	CITATIONS
703	The growth of multi-walled carbon nanotubes with different morphologies on carbon fibers. Carbon, 2005, 43, 663-665.	5.4	118
704	Synthesis and characterization of double-walled carbon nanotubes from multi-walled carbon nanotubes by hydrogen-arc discharge. Carbon, 2005, 43, 623-629.	5.4	64
705	Fractal effects on the measurement of the specific surface areas of single-walled carbon nanotubes. Carbon, 2005, 43, 1785-1787.	5.4	3
706	Preparation of carbon microcoils by catalytic decomposition of acetylene using nickel foam as both catalyst and substrate. Carbon, 2005, 43, 1874-1878.	5.4	35
707	Some indications of the formation mechanism for double-walled carbon nanotubes by hydrogen-arc discharge. Carbon, 2005, 43, 2027-2030.	5.4	7
708	Van der Waals interactions between two parallel infinitely long single-walled nanotubes. Chemical Physics Letters, 2005, 403, 343-346.	1.2	62
709	Synthesis of rectangular cross-section AlN nanofibers by chemical vapor deposition. Chemical Physics Letters, 2005, 416, 171-175.	1.2	34
710	Carbon nanotubes for clean energy applications. Journal Physics D: Applied Physics, 2005, 38, R231-R252.	1.3	101
711	Morphology, thermal stability, and dynamic mechanical properties of atactic polypropylene/carbon nanotube composites. Journal of Applied Polymer Science, 2005, 98, 1087-1091.	1.3	119
712	Fabrication of Low-Voltage Electron Source from Patterned Arrays of Aligned Single-Walled Carbon Nanotube Ropes. Japanese Journal of Applied Physics, 2005, 44, 7713-7716.	0.8	0
713	Positive temperature coefficient effect in multiwalled carbon nanotube/high-density polyethylene composites. Applied Physics Letters, 2005, 86, 062112.	1.5	146
714	KH+Ti co-doped NaAlH4 for high-capacity hydrogen storage. Journal of Applied Physics, 2005, 98, 074905.	1.1	23
715	Field emission properties of macroscopic single-walled carbon nanotube strands. Applied Physics Letters, 2005, 86, 223114.	1.5	43
716	Polarized Raman analysis of aligned double-walled carbon nanotubes. Physical Review B, 2005, 71, .	1.1	22
717	Axial Young's modulus prediction of single-walled carbon nanotube arrays with diameters from nanometer to meter scales. Applied Physics Letters, 2005, 87, 193101.	1.5	47
718	Packing-dependent pore structures in single-walled carbon nanotube arrays. Applied Physics Letters, 2005, 87, 243109.	1.5	5
719	Controlling field-emission patterns of isolated single-walled carbon nanotube rope. Applied Physics Letters, 2005, 87, 043114.	1.5	3
720	Direct formation of Na3AlH6 by mechanical milling NaHâ^•Al with TiF3. Applied Physics Letters, 2005, 87, 071911.	1.5	23

#	Article	IF	CITATIONS
721	Structure and thermal expansion of multi-walled carbon nanotubes before and after high temperature treatment. Journal Physics D: Applied Physics, 2005, 38, 4302-4307.	1.3	74
722	Stability of Supershort Single-Walled Carbon Nanotubes. Journal of Physical Chemistry B, 2005, 109, 12406-12409.	1.2	17
723	An array of Eiffel-tower-shape AlN nanotips and its field emission properties. Applied Physics Letters, 2005, 86, 233104.	1.5	87
724	Light emission and degradation of single-walled carbon nanotube filament. Journal of Applied Physics, 2005, 98, 044306.	1.1	11
725	Field emission from AlN nanorod array. Applied Physics Letters, 2005, 86, 153104.	1.5	91
726	Aligned Double-Walled Carbon Nanotube Long Ropes with a Narrow Diameter Distribution. Journal of Physical Chemistry B, 2005, 109, 7169-7173.	1.2	45
727	Exploration of the Nature of Active Ti Species in Metallic Ti-Doped NaAlH4. Journal of Physical Chemistry B, 2005, 109, 20131-20136.	1.2	84
728	New Insight into the Solid Electrolyte Interphase with Use of a Focused Ion Beam. Journal of Physical Chemistry B, 2005, 109, 22205-22211.	1.2	89
729	Preparation of single-crystal α-MnO2 nanorods and nanoneedles from aqueous solution. Journal of Alloys and Compounds, 2005, 397, 282-285.	2.8	55
730	Effects of SWNT and Metallic Catalyst on Hydrogen Absorption/Desorption Performance of MgH2. Journal of Physical Chemistry B, 2005, 109, 22217-22221.	1.2	102
731	A self-similar array model of single-walled carbon nanotubes. Applied Physics Letters, 2005, 86, 203106.	1.5	7
732	High-performance dual-gate carbon nanotube FETs with 40-nm gate length. IEEE Electron Device Letters, 2005, 26, 823-825.	2.2	107
733	Surface fractal dimension of single-walled carbon nanotubes. Physical Review B, 2004, 69, .	1.1	21
734	Fatigue failure mechanisms of single-walled carbon nanotube ropes embedded in epoxy. Applied Physics Letters, 2004, 84, 2811-2813.	1.5	46
735	SYNTHESIS OF WORMLIKE NANOPOROUS NICKEL OXIDE WITH NANOCRYSTALLINE FRAMEWORK FOR ELECTROCHEMICAL ENERGY STORAGE. International Journal of Nanoscience, 2004, 03, 321-329.	0.4	13
736	The morphology and thermal properties of multi-walled carbon nanotube and poly(hydroxybutyrate-co-hydroxyvalerate) composite. Polymer International, 2004, 53, 1479-1484.	1.6	105
737	Surface modification of single-walled carbon nanotubes with polyethylene viain situ Ziegler-Natta polymerization. Journal of Applied Polymer Science, 2004, 92, 3697-3700.	1.3	84
738	Thermal expansion of a composite of single-walled carbon nanotubes and nanocrystalline aluminum. Carbon, 2004, 42, 3260-3262.	5.4	74

#	Article	IF	CITATIONS
739	Purification of Single-Wall Carbon Nanotubes by Electrochemical Oxidation. Chemistry of Materials, 2004, 16, 5744-5750.	3.2	149
740	SYNTHESIS AND CHARACTERIZATION OF CARBON NANOTUBES FOR HYDROGEN STORAGE. Series on Chemical Engineering, 2004, , 263-316.	0.2	0
741	High-purity single-wall carbon nanotubes synthesized from coal by arc discharge. Carbon, 2003, 41, 2170-2173.	5.4	77
742	Tension–tension fatigue behavior of unidirectional single-walled carbon nanotube reinforced epoxy composite. Carbon, 2003, 41, 2177-2179.	5.4	81
743	Hydrogen adsorption/desorption behavior of multi-walled carbon nanotubes with different diameters. Carbon, 2003, 41, 2471-2476.	5.4	158
744	Observations of novel carbon nanotubes with multiple hollow cores. Carbon, 2003, 41, 2477-2480.	5.4	8
745	Influence of ferrocene/benzene mole ratio on the synthesis of carbon nanostructures. Chemical Physics Letters, 2003, 376, 83-89.	1.2	65
746	Micro-mechanical properties and morphological observation on fracture surfaces of carbon nanotube composites pre-treated at different temperatures. Composites Science and Technology, 2003, 63, 1161-1164.	3.8	68
747	Identification of the constituents of double-walled carbon nanotubes using Raman spectra taken with different laser-excitation energies. Journal of Materials Research, 2003, 18, 1251-1258.	1.2	38
748	Micro-hardness and Flexural Properties of Randomly-oriented Carbon Nanotube Composites. Journal of Composite Materials, 2003, 37, 365-376.	1.2	51
749	Effect of geometrical parameters on the field-emission properties of single-walled carbon nanotube ropes. Journal of Materials Research, 2003, 18, 2188-2193.	1.2	5
750	MICROSTRUCTURE AND RESISTIVITY OF CARBON NANOTUBE AND NANOFIBER/EPOXY MATRIX NANOCOMPOSITE. , 2003, , .		0
751	Fatigue Behaviour of Unidirectional Single-Walled Carbon Nanotube Reinforced Epoxy Composite under Tensile Load. Advanced Composites Letters, 2003, 12, 096369350301200.	1.3	4
752	MECHANICAL PROPERTIES OF SURFACTANT-COATING CARBON NANOFIBER/EPOXY COMPOSITE. , 2003, , .		0
753	Volumetric hydrogen storage in single-walled carbon nanotubes. Applied Physics Letters, 2002, 80, 2389-2391.	1.5	63
754	Boron nitride nanotubes filled with zirconium oxide nanorods. Journal of Materials Research, 2002, 17, 2761-2764.	1.2	15
755	MICROSTRUCTURE AND RESISTIVITY OF CARBON NANOTUBE AND NANOFIBER/EPOXY MATRIX NANOCOMPOSITE. International Journal of Nanoscience, 2002, 01, 719-723.	0.4	6
756	Microwave Electromagnetic Characteristics of a Microcoiled Carbon Fibers/paraffin Wax Composite in Ku Band. Journal of Materials Research, 2002, 17, 1232-1236.	1.2	62

#	Article	IF	CITATIONS
757	Bulk Storage Capacity of Hydrogen in Purified Multiwalled Carbon Nanotubes. Journal of Physical Chemistry B, 2002, 106, 963-966.	1.2	64
758	Electrochemical Hydrogen Storage Behavior of Ropes of Aligned Single-Walled Carbon Nanotubes. Nano Letters, 2002, 2, 503-506.	4.5	103
759	MECHANICAL PROPERTIES OF SURFACTANT-COATING CARBON NANOFIBER/EPOXY COMPOSITE. International Journal of Nanoscience, 2002, 01, 425-430.	0.4	15
760	Morphology, diameter distribution and Raman scattering measurements of double-walled carbon nanotubes synthesized by catalytic decomposition of methane. Chemical Physics Letters, 2002, 359, 196-202.	1.2	139
761	Hydrogen storage in carbon nanotubes. Carbon, 2001, 39, 1447-1454.	5.4	532
762	Purification of single-walled carbon nanotubes synthesized by the hydrogen arc-discharge method. Journal of Materials Research, 2001, 16, 2526-2529.	1.2	140
763	Solid catalytic growth mechanism of micro-coiled carbon fibers. Science in China Series D: Earth Sciences, 2001, 44, 377-382.	0.9	10
764	Evaluation of diameter distribution of inside cavities of open CNTs by analyses of nitrogen cryo-adsorption isotherm. Science Bulletin, 2001, 46, 1317-1320.	1.7	5
765	Adsorption and capillarity of nitrogen in aggregated multi-walled carbon nanotubes. Chemical Physics Letters, 2001, 345, 18-24.	1.2	213
766	The influence of preparation parameters on the mass production of vapor-grown carbon nanofibers. Carbon, 2000, 38, 789-795.	5.4	51
767	Tailoring the diameters of vapor-grown carbon nanofibers. Carbon, 2000, 38, 921-927.	5.4	44
768	Identification of the conducting category of individual carbon nanotubes from Stokes and anti-Stokes Raman scattering. Physical Review B, 2000, 62, 5186-5190.	1.1	29
769	Polarized Raman Study of Single-Wall Semiconducting Carbon Nanotubes. Physical Review Letters, 2000, 85, 2617-2620.	2.9	221
770	Tensile strength of single-walled carbon nanotubes directly measured from their macroscopic ropes. Applied Physics Letters, 2000, 77, 3161-3163.	1.5	306
771	A TEM study of microstructure of carbon fiber/polycarbosilane-derived SiC composites. Carbon, 1999, 37, 2057-2062.	5.4	56
772	Hydrogen uptake in vapor-grown carbon nanofibers. Carbon, 1999, 37, 1649-1652.	5.4	173
773	Title is missing!. Journal of Materials Science, 1999, 34, 827-834.	1.7	32
774	Graphitization Behavior of Wood Ceramics and Bamboo Ceramics as Determined by X-Ray Diffraction. Journal of Porous Materials, 1999, 6, 233-237.	1.3	63

#	Article	IF	CITATIONS
775	Hydrogen Storage in Single-Walled Carbon Nanotubes at Room Temperature. Science, 1999, 286, 1127-1129.	6.0	1,795
776	Large-scale and low-cost synthesis of single-walled carbon nanotubes by the catalytic pyrolysis of hydrocarbons. Applied Physics Letters, 1998, 72, 3282-3284.	1.5	678
777	Preparation, morphology, and microstructure of diameter-controllable vapor-grown carbon nanofibers. Journal of Materials Research, 1998, 13, 2342-2346.	1.2	69
778	Preparation and Fracture Behavior of Carbon Fiber/SiC Composites by Multiple Impregnation and Pyrolysis of Polycarbosilane. Journal of the Ceramic Society of Japan, 1998, 106, 1155-1161.	1.3	19
779	Effect of silicon additions on characteristics of carbon fiber reinforced aluminum composites during thermal exposure. Journal of Materials Research, 1996, 11, 1284-1292.	1.2	11
780	Characteristics of several carbon fibrereinforced aluminium composites prepared by a hybridization method. Journal of Materials Science, 1994, 29, 4342-4350.	1.7	16
781	Microstructure of Silicon Nitride Ceramics and Morphology of Surface Damage Induced by Round Indenter. Journal of the Ceramic Society of Japan, 1994, 102, 350-354.	1.3	1
782	Effect of SiO <sub>2</sub> Type and Additives on the Reaction Products in SiO <sub>2</sub> -Al-C-N <sub>2</sub> System. Journal of the Ceramic Society of Japan, 1994, 102, 675-679.	1.3	0
783	Oxidation of Carbon/B <sub>4</sub> C/SiC/ZrB <sub>2</sub> Composite in Moist Air at Elevated Temperature and the Thermodynamic Consideration. Journal of the Ceramic Society of Japan, 1994, 102, 925-929.	1.3	1
784	Preparation of carbon fibre reinforced aluminium via ultrasonic liquid infiltration technique. Materials Science and Technology, 1993, 9, 609-614.	0.8	14
785	Behaviour of carbon fibre reinforced Al–Si composites after thermal exposure. Materials Science and Technology, 1992, 8, 275-282.	0.8	8
786	Fabrication of carbon fibre-reinforced aluminium composites with hybridization of a small amount of particulates or whiskers of silicon carbide by pressure casting. Journal of Materials Science, 1992, 27, 3617-3623.	1.7	23
787	Hybridization with SiC particulates to control the fibre volume fraction and improve the longitudinal tensile strength of carbon fibre-reinforced aluminium composites. Journal of Materials Science Letters, 1991, 10, 795-797.	0.5	10
788	Dissolution–Precipitation Dynamics in Ester Electrolyte for High-Stability Lithium Metal Batteries. ACS Energy Letters, 0, , 1413-1421.	8.8	50
789	FeCl3-functionalized graphene oxide/single-wall carbon nanotube/silicon heterojunction solar cells with an efficiency of 17.5%. Journal of Materials Chemistry A, 0, , .	5.2	9
790	Resonant Scattering in Proximity oupled Graphene/Superconducting Mo <sub>2</sub> C Heterostructures. Advanced Science, 0, , 2201343.	5.6	1